# Error Crafting in Mixed Quantum Gate Synthesis

Nobuyuki Yoshioka, 1, 2, 3, 4, \* Seiseki Akibue, 5 Hayata Morisaki, 6 Kento Tsubouchi, 1 and Yasunari Suzuki 1 Department of Applied Physics, University of Tokyo, 7-3-1 Hongo, Bunkyo-ku, Tokyo 113-8656, Japan 2 Theoretical Quantum Physics Laboratory, RIKEN Cluster for Pioneering Research (CPR), Wako-shi, Saitama 351-0198, Japan 3 JST, PRESTO, 4-1-8 Honcho, Kawaguchi, Saitama, 332-0012, Japan 4 International Center for Elementary Particle Physics, University of Tokyo, 7-3-1 Hongo, Bunkyo-ku, Tokyo 113-0034, Japan 5 NTT Communication Science Laboratories, NTT Corporation, Atsugi 243-0198, Japan 6 Graduate School of Engineering Science, Osaka University 1-3 Machikaneyama, Toyonaka, Osaka 560-8531, Japan 7 NTT Computer and Data Science Laboratories, NTT Corporation, Musashino 180-8585, Japan

In fault-tolerant quantum computing, errors in unitary gate synthesis is comparable with noise inherent in the gates themselves. While mixed synthesis can suppress such coherent errors quadratically, there is no clear understanding on its remnant error, which hinders us from designing a holistic and practical error countermeasure. In this work, we propose that the classical characterizability of synthesis error can be exploited; remnant errors can be crafted to satisfy desirable properties. We prove that we can craft the remnant error of arbitrary single-qubit unitaries to be Pauli and depolarizing errors, while the conventional twirling cannot be applied in general. For Pauli rotation gates, in particular, the crafting enables us to suppress the remnant error up to cubic order, which results in synthesis with a T-count of  $\log_2(1/\varepsilon)$  up to accuracy of  $\varepsilon = 10^{-9}$ . Our work opens a novel avenue in quantum circuit design and architecture that orchestrates error countermeasures.

#### INTRODUCTION

It is widely accepted that quantum computers with error correction [1, 2] can be potentially useful in various tasks such as factoring [3], quantum many-body simulation [4], quantum chemistry [5], and machine learning [6]. With the tremendous advancements in quantum technology, the earliest experimental demonstrations of quantum error correction are realized with various codes [7– 15]. While such progress towards fault-tolerant quantum computing (FTQC) is promising, quantum computers in the coming generation, the early fault-tolerant quantum computers, would still be subject to noise at the logical level, and hence the error countermeasures developed for noisy intermediate-scale quantum (NISQ) devices, in particular the quantum error mitigation (QEM) techniques [16-23], will remain essential to exemplify practical quantum advantage [24–30]. Meanwhile, there is a stark difference between (early) FTQC and NISQ regimes that is characterized by the Eastin-Knill theorem [31]; currently known FTQC schemes are based on universal gate sets that consist of discrete gates. This indicates that the gate synthesis yields coherent error whose effect is comparable to incoherent errors triggered by noise in the hardware.

In contrast to incoherent errors which inevitably necessitate entropy reduction via measurement and feedback [32–35], there is no corresponding fundamental limitation for coherent errors. In fact, several previous works have found that algorithmic errors can be dealt with more efficiently than naive expectation [36–41]. It was pointed out by Refs. [36, 37] that, when one has access to a Pauli rotation exposed to over and under rotations, we can simply take a classical mixture of two to achieve quadratic suppression of the error. Such findings have invoked the

proposal of a mixed synthesis scheme that approximately halves the consumption of magic gates under single-qubit unitary synthesis [39, 41]. It must be noted that, these existing works merely focus on the accuracy of the mixed synthesis, while one must take care of the compatibility between other error countermeasures to further suppress the errors. This is prominent when one desires to obtain unbiased estimator via the QEM, which requires a deep knowledge of the error channel. To our knowledge, however, there is no firm understanding on the remnant error channel nor attempt to control the profile of them.

In this work, we make a first step to fill this gap by introducing a notion of error crafting, i.e., perform the mixed synthesis that results in a remnant error channel with a desired property, for single-qubit unitaries synthesized under the framework of Clifford+T formalism. We rigorously prove that one can design a synthesis protocol that ensures the remnant error is constrained to Pauli error, which is crucial to perform efficient error mitigation techniques [16, 17, 25]. We further provide numerical evidence that, in the case of Pauli rotation gates, one can reliably manipulate the remnant error to be biased. This allows us to perform error detection at the logical level which achieves quadratically small sampling overhead compared to the existing lower bound of sample complexity that does not rely on mid-circuit measurement [33]. We furthermore extend our framework to perform error crafting using CPTP channels obtained from error correction at the logical layer, and show that the remnant error can be suppressed up to cubic order. As a result, we can implement Pauli rotation gates of accuracy  $\varepsilon$  with T-count of  $\log_2(1/\varepsilon)$  up to  $\varepsilon = 10^{-9}$ , which is expected to be sufficient for various medium-scale FTQC beyond state-of-the-art classical computation [26–28, 30].

We remark that the operation of twirling shares the

	Pauli twirl	Clifford twirl	Crafting
T gate	✓	Partially	<b>√</b>
Z rotation	Partially	Partially	✓
Arbitrary	×	×	✓

TABLE I. Applicability of noise shaping techniques for unitary synthesis error in single-qubit non-Clifford gates. The row "T gate" represents the applicability for all single-qubit gates from the third level of the Clifford hierarchy. Of course, the synthesis error is not present if one includes the T gate in the implementable operations, since there is no need for crafting. The row "Z rotation" represents the applicability for Pauli rotation gates. Here, "Partially" means that we can employ a symmetric Clifford group that commutes with the target unitary to twirl the noise within each irreducible representation but not the entire space [44, 45]. For instance, over- and under-rotation errors cannot be twirled; one must rely on crafting.

spirit, since it also transforms a noise channel into another channel with better-known properties via randomized gate compilation. However, there are two severe limitations in twirling: first, it agnostically smears out the characteristics of the channel, and second, it cannot ensure the noise maps to be stochastic when one considers non-Clifford operations beyond the third level of Clifford hierarchy (see Table I and Supplementary Note S1 for details). We note that existing works on randomized compiling report suppression of the noise [38, 42, 43], while we are not aware of any work that guarantees the structure of the noise channel. This is in sharp contrast to our work, since our objective is to fully utilize the information on the error profile of general unitary synthesis that can be characterized completely and efficiently via classical computation.

#### RESULTS

#### Unitary, mixed, and error-crafted synthesis

We aim to implement a target single-qubit unitary  $\hat{U}$  with its channel representation given by  $\hat{\mathcal{U}}$ . We hereafter distinguish the unitaries before and after synthesis by the presence and absence of a hat. Due to the celebrated Eastin-Knill's theorem [31], there is no fault-tolerant implementation of continuous gate sets, and therefore we cannot exactly implement the target in general. We alternatively aim to approximate  $\hat{U}$  by decomposing it to a sequence of implementable operations. Such a task is called gate synthesis.

One of the most common approaches for gate synthesis is the unitary synthesis, namely to decompose the target unitary into a sequence of implementable unitary gate sets. For instance, unitary synthesis into the Clifford+T gate set is known to be possible with classical computation time of  $O(\text{polylog}(1/\epsilon))$  for arbitrary single-qubit Pauli rotation assuming a factoring oracle [46] and

 $O(\text{poly}(1/\epsilon))$  for a general SU(2) gate [47, 48]. Another measure for the efficiency of synthesis is the number of T gates, or the T-count, since T gates require cumbersome procedures such as magic state distillation and gate teleportation. In this regard, the existing methods nearly saturates the information-theoretic lower bound regarding the T-count of  $3\log_2(1/\epsilon)$  except for rare exceptions that require  $4\log_2(1/\epsilon)$  [46–49].

We may also consider mixed synthesis, which takes a classical mixture of several different outputs from the unitary synthesis algorithm. Concretely, we generate a set of slightly shifted unitaries  $\{U_j\}$  which are  $\epsilon$ -close approximations of the target unitary  $\hat{U}$  in terms of diamond distance as  $d_{\diamond}(\hat{\mathcal{U}},\mathcal{U}_j) \leq \epsilon$  (see Supplementary Note S2 for the definition of diamond distance). It is known that the mixed synthesis allows quadratic suppression of the error, when we appropriately generate a set of synthesized unitaries  $\{\mathcal{U}_j\}$  and choose the probability distribution over them:

**Lemma 1.** (informal [41]) Let  $\hat{U}$  be a target unitary channel with  $\{U_j\}$  constituting its  $\epsilon$ -net in terms of the diamond distance. Then, one can find the optimal weight  $\{p_j\}$  such that the diamond distance is bounded as

$$d_{\diamond}\left(\hat{\mathcal{U}}, \sum_{j} p_{j} \mathcal{U}_{j}\right) \leq \epsilon^{2},$$
 (1)

by solving the following minimization problem via semidefinite programming:

$$p = \underset{p}{\operatorname{argmin}} \ d_{\diamond} \left( \hat{\mathcal{U}}, \sum_{j} p_{j} \mathcal{U}_{j} \right). \tag{2}$$

As an extension of existing synthesis techniques, here we propose *error-crafted synthesis*, or *error crafting*. In short, this can be understood as constraining the remnant error of the synthesis, depending on the subsequent error countermeasure (such as QEM or error detection) one wishes to perform. We formally define the remnant error channel as

$$\mathcal{E}_{\text{rem}}(\cdot) = \left(\sum_{j} p_{j} \Lambda_{j}\right) \circ \hat{\mathcal{U}}^{-1}(\cdot) = \sum_{ab} \chi_{ab} P_{a} \cdot P_{b}, \quad (3)$$

where  $P_a \in \{I, X, Y, Z\}$  and  $\{\chi_{ab}\}$  gives the chi representation of the remnant error. We also allow the implementable channel to be a non-unitary CPTP map as  $\{\Lambda_j\}$ , which we find to be useful when we incorporate measurement and feedback as discussed later. The aim of the crafted synthesis is to control  $\{\chi_{ab}\}$  by optimizing the probability distribution  $\{p_j\}$  for appropriately generated  $\{\Lambda_j\}$ .

Let us remark that we require the synthesis protocol to be distinct from the QEM stage, in a sense that we do not allow synthesis to increase the sampling overhead, the multiplication factor in the number of circuit execution. Also, we require that the gate complexity is nearly homogeneous even if we include feedback operations, in order to prevent a situation where parallel application of multiple synthesized channels is stalled due to a fallback scheme [39, 50].

#### Crafting remnant error to be Pauli channel

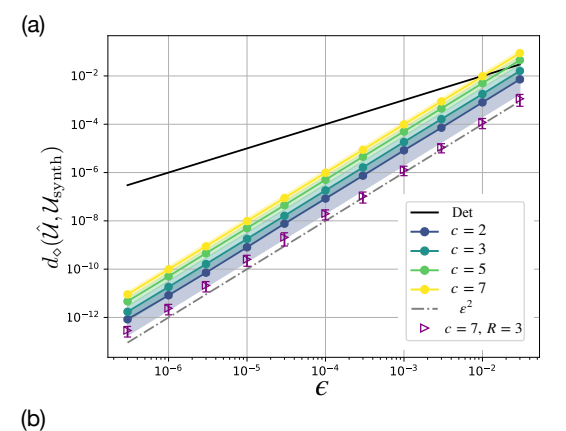
While the quadratic suppression (1) by mixed synthesis is already beneficial for practical quantum computing, the performance of many error counteracting protocols can be enhanced when we craft the remnant error  $\mathcal{E}_{\text{rem}}$ . For instance, let us consider the probabilistic error cancellation (PEC), which is one of the most well-known error mitigation techniques that estimate expectation values of physical observables by the quasi-probabilistic implementation of error channel inversion [16, 51]. One can show that it suffices to take Clifford operations and Pauli initialization to constitute a universal set to invert arbitrary single-qubit error channels [18, 52], while the implementation is significantly simplified when  $\mathcal{E}_{rem}$  is a Pauli channel. This is because the PEC can be performed merely via updates on Pauli frames, which is purely done by classical processing of stabilizer measurements [25]. As another example, when we consider the rescaling technique under white-noise approximation [53, 54], which is a provably cost-optimal way of error mitigation, we can drastically improve the accuracy of the approximation when the errors are free from coherent components (see Supplementary Note S6 for details).

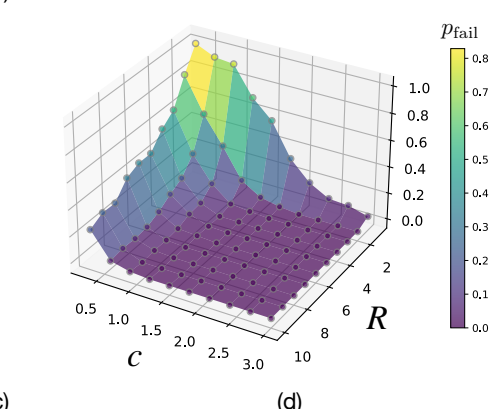
In this regard, we make a further step and ask the following question: can we guarantee both quadratic error suppression and success of crafting the remnant error to be Pauli channel? This is equivalent to solving the following optimization problem:

minimize 
$$d_{\diamond}\left(\hat{\mathcal{U}}, \sum_{j} p_{j} \mathcal{U}_{j}\right)$$
 s.t.  $\mathcal{E}_{\text{rem}}(\cdot) = \sum_{a} \chi_{aa} P_{a} \cdot P_{a}$ , (4)

where  $\chi_{aa} \geq 0$  is required for all a. We emphasize that this cannot be achieved by naively applying twirling techniques, since randomization for coherent errors following non-Clifford unitary demands non-Clifford operations, which are not error-free in FTQC (see Supplementary Note S1). Our strategy is to prepare shift unitaries  $\{\mathcal{V}_{j}^{c\epsilon}\}_{j}$  that can be used to generate a set of  $c\epsilon$ -close unitaries such that the feasibility of the minimization problem (4) is guaranteed, even when unitary synthesis induces error of  $\epsilon$ . By explicitly constructing such a set of shift unitaries, we rigorously answer to the above-raised question as the following:

**Theorem 1.** There exist shift factor c, a positive number  $\epsilon_0$ , and a set of shift unitaries  $\{\mathcal{V}_j^{c\epsilon}\}_{j=1}^7$  such that, for any given single-qubit unitary  $\hat{\mathcal{U}}$  and for any  $\epsilon \in (0, \epsilon_0]$ , if we synthesize the shifted target unitaries to obtain





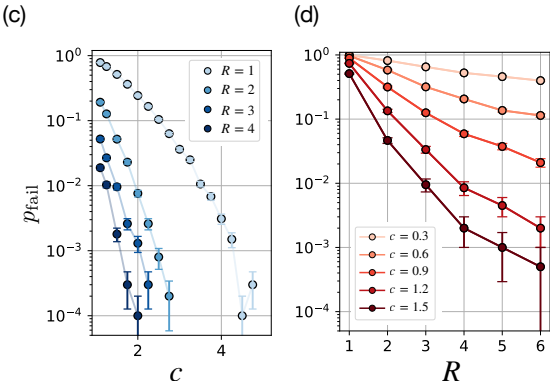


FIG. 1. Numerical analysis on error-crafted synthesis for the Pauli constraint. (a) Diamond distance  $d_{\diamond}(\mathcal{U}, \mathcal{U}_{\text{synth}})$  between the target single-qubit Haar random unitary  $\hat{\mathcal{U}}$  and the synthesized channel  $\mathcal{U}_{\text{synth}} := \sum_{i} p_{i} \mathcal{U}_{i}$ . The black real line indicates the results from unitary synthesis by the Ross-Selinger algorithm, while the filled dots are results from mixed synthesis with shift factors of c = 2, 3, 5, 7. When we increase the number of synthesized unitaries by a factor of R = 3 (see main text for detailed definition) for c=7, shown by unfilled triangles, the remnant synthesis error is suppressed below the bound in Eq. (5) and approaches the value of  $\epsilon^2$ , which matches the upper bound for the nonconstrained case as in Eq. (1). The plots are averaged over 200 random instances of target unitaries. (b) Surface plot of failure rate  $p_{\text{fail}}$  of mixed synthesis under the Pauli constraint, averaged over 200 instances for  $\epsilon = 10^{-4}$ . Scaling with c and R are shown in (c), (d), where the number of instances is 10000 and 2000, respectively.

 $\{\mathcal{U}_j\} = \{\mathcal{A}(\mathcal{V}_j^{c\epsilon} \circ \hat{\mathcal{U}})\}$  so that  $d_{\circ}(\mathcal{V}_j^{c\epsilon} \circ \hat{\mathcal{U}}, \mathcal{U}_j) \leq \epsilon$  is satisfied under the synthesis algorithm  $\mathcal{A}$ , then there exists a mixture of  $\{\mathcal{U}_j\}$  that induces a Pauli channel as the effective synthesis error, with the accuracy being

$$(c-1)^2 \epsilon^2 \le d_{\diamond} \left( \hat{\mathcal{U}}, \sum_j p_j \mathcal{U}_j \right) \le (c+1)^2 \epsilon^2.$$
 (5)

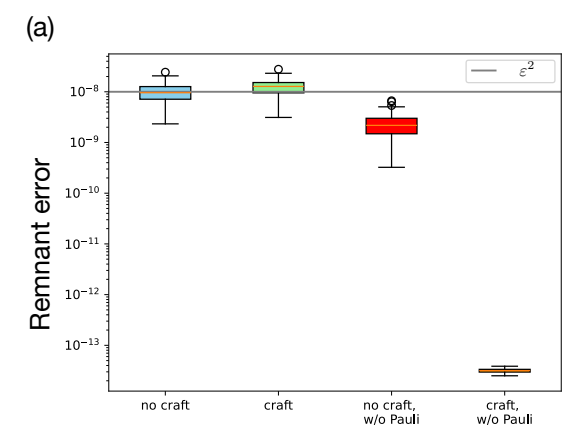
Remarkably, this theorem states that we can craft the error without assuming anything but the accuracy for the synthesis algorithm  $\mathcal{A}$ . It is also worth noting that the minimization problem (4) can be solved by the linear programming.

To prove Theorem 1, we explicitly construct the shift unitaries  $\{\mathcal{V}_j^{c\epsilon}\}_j$ , and show that the feasibility of the solution is robust even under additional synthesis error of  $\epsilon$ . Once such a solution is ensured, the upper bound of Eq. (5) follows directly from the formulation via the minimization over diamond distance and the fact that  $\{\mathcal{U}_j\}_{j=1}^7$  is  $(c+1)\epsilon$ -close to  $\hat{\mathcal{U}}$  with respect to the diamond distance. Also, the lower bound follows from the fact that the diamond distance between the compiled shifted unitaries  $\{\mathcal{U}_j\}$  and the target unitary  $\hat{\mathcal{U}}$  are at least  $(c-1)\epsilon$ . We guide readers to Supplementary Note S7 for details of the proof.

Since the theorem only states the existence of finite c, we rely on numerical simulation to verify the practical usage with finite c values. For this purpose, we synthesize a single-qubit Haar random unitary gate by first performing the axial decomposition into three Pauli rotations, each of which passed to the synthesis algorithm proposed by Ross and Selinger [46]. As shown in Fig. 1(a), the mixed synthesis indeed yields error-bounded solutions that achieve quadratic suppression compared to the unitary synthesis. Meanwhile, we find that the Pauli constraint is violated when we take small shift factors c. This is not contradicting Theorem 1, since the theorem only states the existence of c which always yield successful results. It must be noted that, as shown in Fig. 1(b) and (c), the occurrence of such a violation is suppressed exponentially by increasing the value of c. We observe that it suffices to take  $c \sim 3.5, 4.5$  to yield feasible solution with failure probability of  $10^{-2}$ ,  $10^{-3}$ , respectively, and naturally deduce that  $c \sim 5.5, 6.5$  is required to reach  $10^{-4}$ ,  $10^{-5}$ . We remark that, while we have employed the axial decomposition of the SU(2) gates for the results shown here, we observe similar suppression when we utilize a direct synthesis algorithm [55].

Since increasing the shift factor c increases the prefactor of the remnant error by  $c^2$ , we find it beneficial to introduce another practical strategy that enhances the feasibility of the solution. Here we provide a simple yet powerful technique; by generating the shift unitaries for R different shift factors c/R, 2c/R, ..., c and solving the problem (4) with R-fold larger number of basis set, we can both suppress the failure of error-crafted synthesis (see Fig. 1(b) and (d)) and the remnant error. As shown in Fig. 1(a), when we take c = 7 and R = 3, we

find that the diamond distance is suppressed as  $\epsilon^2$  for a broad range of the synthesis accuracy  $\epsilon$ , which is a significant improvement from the case of R=1 with  $\sim c^2\epsilon^2$ . Note that this is extremely beneficial when we wish to eliminate such remnant errors using QEM methods. To be concrete, the sampling overhead is given as  $(1+4p)^L$  under error rate of p with L gates when one employs the PEC method, and hence the reduction of the remnant error from  $p_{\rm rem} \sim c^2\epsilon^2$  to  $p_{\rm rem} \sim \epsilon^2$  results in exponential difference with L. For instance, when we implement  $\{1,2,3\} \times 10^8$  rotation Pauli gates with  $\epsilon=10^{-5}$ , the sampling overhead is reduced by factors of 6.8, 47, and 317, respectively.



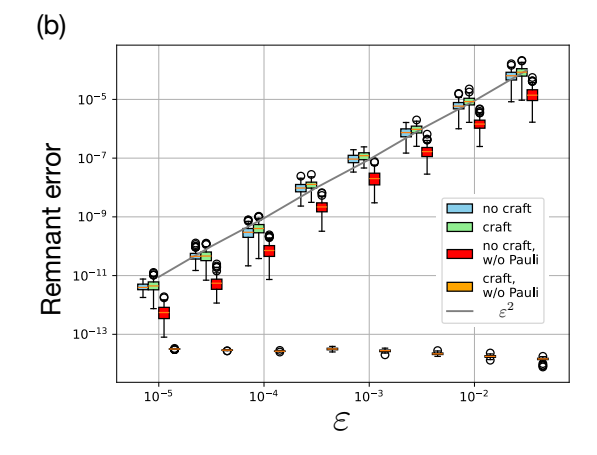


FIG. 2. Comparison of the magnitude of remnant errors  $d_{\diamond}(\mathcal{E}_{\text{rem}}, \mathcal{I})$ . (a) Box plots are provided for the magnitude of remnant errors of 100 random instances of Z rotation gate, with unitary synthesis done for  $\epsilon = 10^{-4}$ . The left two box plots show  $d_{\diamond}(\mathcal{E}_{\text{rem}}, \mathcal{I})$  with and without crafting for Pauli error, and the right two box plots indicate the magnitude of the non-Pauli contribution. (b) Scaling of the remnant errors with  $\epsilon$ . In both panels, shift unitaries are generated with c = 3, R = 5.

We remark that crafting is actually essential to guarantee the remnant channel to be a Pauli channel. In Fig. 2, we compare the remnant errors in crafted and uncrafted mixed synthesis. We find that, as expected, the magnitude of the remnant error is slightly smaller when we do

not craft it. However, we can see there is a drastic difference in the non-Pauli component. Here, we calculate the magnitude of the error that persists even after we eliminate the Pauli component as  $\min_{\mathcal{R}} d_{\diamond}(\mathcal{R} \circ \mathcal{E}_{\text{rem}}, \mathcal{I})$ , where  $\mathcal{R}$  is minimized over the set of trace-preserving maps that inverts Pauli error. We can see that the non-Pauli component in uncrafted synthesis remains as  $O(\epsilon^2)$ , while in the crafted synthesis the magnitude is suppressed below  $10^{-13}$ . We attribute this residual to the relaxation of equality constraint into inequality, which was performed to enhance the stability of the numerical solver (see Supplementary Note S3). While we show the result for Z rotation here, we have confirmed that similar results can be obtained for general SU(2) gates as well.

As another practical remark, note that the number of bases with nonzero probability  $(\sum_{p_j\neq 0}1)$  is always upper-bounded by 10. Hence, the actual memory footprint of the transpiled circuit is comparable to ordinary mixed synthesis algorithms.

#### Crafting remnant error to be detectable

If one chooses to employ the PEC method as the QEM method for FTQC, it suffices to guarantee only the feasibility under the Pauli constraint. Indeed, the PEC method is powerful in the sense that one may perform unbiased estimation when the error channel is precisely known. However, we find that the remnant errors can be counteracted much more effectively by utilizing the fact that they can be characterized completely by classical computation. For instance, we may wish to craft local depolarizing errors, since many limits and performance of quantum algorithms, as well as QEM methods, are analyzed under the assumption of the local depolarizing noise [19, 32, 35, 56, 57]. We may alternatively wish to craft the remnant errors to be some biased Pauli noise. We find that this is extremely beneficial for the case of the Pauli rotation gates. Namely, we can perform error detection or correction in the *logical* layer, which reduces the sampling overhead to the extent that QEM methods designed for general channels cannot achieve.

First, let us discuss the crafting of the depolarizing channel. Following a similar strategy as in Theorem 1, we can mathematically prove that there exists a set of shift unitaries  $\{\mathcal{V}_j^{c\epsilon}\}$  such that we can achieve quadratic suppression of error under the depolarizing constraint, with the sole difference being that the number of shift unitaries is 9 instead of 7. The formal statement and the proof are provided in Supplementary Note S7. Our numerical simulation also shows similar favorable properties as seen in the case of Pauli constraint (See Supplementary Note S3).

Next, let us consider crafting the remnant error to be biased. In particular, we focus on the Pauli Z rotation gate and aim to bias the error to be XY error, since it can be detected using a single ancilla qubit with less sampling overhead than the lower bound for QEM methods that

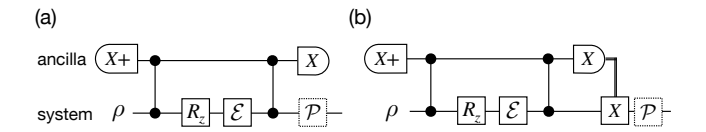


FIG. 3. Circuit structure for (a) error detection and (b) logical error correction for Pauli Z rotation gate  $R_z$  with remnant error of  $\mathcal{E}_{\text{rem}}$ . We may further combine with the PEC method, for which the Pauli operation  $\mathcal{P}$  with dotted square is executed virtually via updating the Pauli frame. Note that the feedback operation in (b) is also done via the Pauli frame.

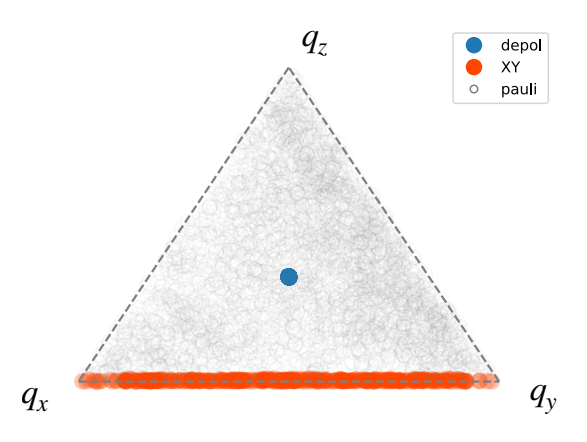


FIG. 4. Numerical analysis on error crafting for remnant errors. Here we display the distribution of error rate ratio  $(q_x,q_y,q_z) \coloneqq (\frac{p_x}{p},\frac{p_y}{p},\frac{p_z}{p})$  on a plane  $q_x+q_y+q_z=1$ , where  $p_a \coloneqq \chi_{aa}$   $(a \in \{x,y,z\})$  is the rate of each Pauli channel in  $\mathcal{E}_{\text{rem}}$  and  $p \coloneqq p_x+p_y+p_z=O(\epsilon^2)$  corresponds to the total error rate. Note that here we show results whose violation of the constraints are below threshold values (see Supplementary Notes S3 for details). The unitary synthesis is done for  $\epsilon=10^{-4}$  with shift factor c=2.0,5.0 for depolarizing and XY constraints, respectively.

do not rely on mid-circuit measurement [33] (concrete circuit structure provided in Fig. 3). While we have not found a guaranteed set of shift unitaries, we find that the nine shift unitaries for the depolarizing noise are of practical use, if we allow violation of the constraint as  $p_z \leq 0.01p$  where  $p := p_x + p_y + p_z$  (see Supplementary Notes S3 for details).

The success of error crafting is highlighted in Fig. 4. As can be seen from Fig. 4(a), while the rate of Pauli errors  $(\frac{p_x}{p}, \frac{p_y}{p}, \frac{p_z}{p})$  is distributed quite homogeneously if we do not impose any constraint on the error profile, we find that the constraints can be reflected with high accuracy. We verify that  $p_x = p_y = p_z$  is satisfied up to the order of machine precision for the depolarizing constraint, while for the XY-biased noise, we find that we cannot completely eliminate the Z error; there is a small residual component of  $p_z = O(\epsilon^3)$  even if we allow the XY-biased noise to consist of non-unital components. We also attempted to craft X-biased noise, while it did not succeed in most instances.

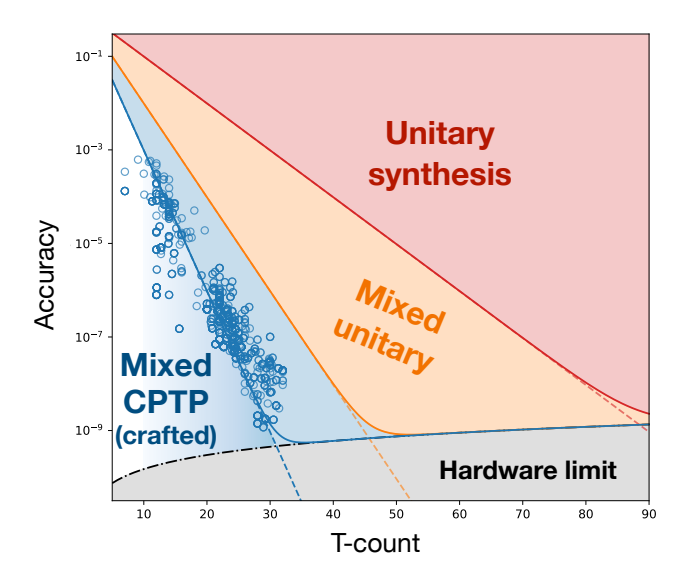


FIG. 5. Trade-off between T-count and synthesis accuracy for Pauli rotation gates. The red, yellow, and blue regions indicate the achievable accuracy without any sampling overhead when we employ unitary, mixed, and error-crafted synthesis. The blue circles indicate the error solely from crafted synthesis for  $R_z(\theta)$  with  $\theta \in \{\frac{m\pi}{32}\}_{m\neq 0 \mod 4}$  under various synthesis accuracy. Note that total error combined with hardware noise is bounded by the chained black line, which indicates the contribution from noise in T gates. Here we choose error rate of  $10^{-11}$  per T gate. The dotted red, yellow, and green lines are given by the empirical T-count of  $3\log_2(1/\varepsilon)$ ,  $1.5\log_2(1/\varepsilon)$ , and  $\log_2(1/\varepsilon)$ , respectively, and the real lines indicate the total error.

# Error crafting using CPTP maps

While we have considered the error crafting using synthe sized unitaries  $\{U_i\}$ , we can also apply the framework to CPTP maps. As a demonstration, here we consider the target unitary  $\hat{U}$  to be a Pauli Z rotation, and constitute the set of implementable CPTP maps  $\{\Lambda_i\}$  as the channels of synthesized unitaries accompanied with entangled measurement and feedback as shown in Fig. 3(b). We have numerically found that, the remnant error can be suppressed *cubically* small as  $\epsilon^3$ , as opposed to the quadratic suppression realized in the error crafting for unitaries. Since the optimal unitary synthesis yield Tcount of  $3\log_2(1/\epsilon) + O(1)$ , such an improvement allows us to synthesize a Pauli rotation gate with a T-count of  $\log_2(1/\varepsilon) + O(1)$  on average. Compare this with the scaling of  $1.5\log_2(1/\varepsilon)$  realized by mixed synthesis, which achieve quadratic improvement in  $\varepsilon$  (see Fig. 5). We guide the readers to the Supplementary Note S4, S5 for a detailed discussion on the search for appropriate  $\Lambda_i$ .

Even if the Z error cannot be eliminated completely, such an error crafting drastically alters the sampling overhead. By performing the error detection operation as shown in Fig. 3(a), we can mitigate Pauli X and Y errors with sampling overhead of  $\gamma_{XY} = 1 + p_x + p_y$ , which is even below the lower bound of QEM sampling over-

head that does not rely on mid-circuit measurement [33]. While the Z error is undetectable and hence we shall rely on other QEM methods such as PEC or rescaling with overhead of  $\gamma_Z = 1 + \alpha p_z$ , the total sampling overhead is  $\gamma_{\text{tot}} = \gamma_{\text{XY}} \gamma_Z \sim 1 + p_x + p_y + \alpha p_z \sim 1 + \epsilon^2$ . When we perform QEM for L gates, the total sampling overhead  $\gamma_{\text{tot}}^L$  is quartically small compared to that of PEC.

An intuitive understanding of the reduction of the T-count can be obtained from a geometric interpretation. Let us first briefly describe the standard volume argument [59] for SU(2) synthesis to yield scaling of  $3\log_2(1/\varepsilon) + O(1)$ , and then proceed to explain the improved scaling of  $\log_2(1/\varepsilon) + O(1)$ . We can interpret the problem of designing a synthesis algorithm, i.e., ensuring any d-dimensional unitary to be approximated by accuracy of  $\varepsilon$ , as packing  $\epsilon$ -ball into the manifold of SU(d). The volume of  $\varepsilon$ -ball in  $(d^2-1)$ -dimensional space is  $O(\varepsilon^{d^2-1})$ , in particular  $V = O(\varepsilon^3)$  for SU(2). Hence, in order to cover the entire space, we need at least  $O(1/V) = O(1/\varepsilon^3)$  unique unitaries. Note that any Clifford+T gate can be expressed uniquely by the canonical form proposed by Matsumoto and Amano [60]. Specifically, the number of unique Clifford+T operator with T-count of t is  $192 \cdot (3 \cdot 2^t - 2)$ . We therefore deduce that the lower bound of T-count scales as  $3\log_2(1/\varepsilon) + O(1)$ . It has been numerically verified that this bound is indeed nearly saturated by a direct search algorithm [55], which reflects the fact that the grid points corresponding to Clifford+T unitary are distributed homogeneously within the manifold so that the gate set quickly mimics the Haar unitary ensemble [61].

When we perform the mixed CPTP synthesis, since we can correct coherent error of X rotation via the feedback operation, we may allow it to be arbitrarily large. This effectively projects out one of the dimensions of the manifold to be covered. Correspondingly, the volume of the ball is regarded as  $V = O(\varepsilon^2)$ . From the volume argument, this leads to the T-count of  $2\log_2(1/\varepsilon) + O(1)$  for the synthesis of unitaries to be included in the mixture. By combining with the fact that appropriate mixed synthesis allows quadratic suppression of error and hence reduces the T-count by a factor of two, we arrive at the scaling of  $\log_2(1/\varepsilon) + O(1)$ .

Let us briefly comment on the classical precomputation time of crafted synthesis. Our results in Fig. 5 exploits the direct search algorithm for SU(2) gate synthesis whose computational complexity scales as  $O(1/\epsilon)$  on average [55]. Considering that currently known unitary synthesis algorithms for  $R_z$  gates based on numbertheoretic approach [46, 62] or repeat-until-success circuits [39, 50] yield nearly optimal gate sequence with computational complexity of  $O(\text{polylog}(1/\epsilon))$ , the complexity of direct search algorithms seems to be a significant overhead. Meanwhile, we observe that the actual computation time per synthesis is observed to be milliseconds for the accuracy regime we have investigated. Considering that such computations can be embarrassingly parallelized, and also that number of rotation gates

Gate	Synthesis	Crafted?	Remnant error		QEM method	Sampling overhead	Comment
Gate			magnitude	type	QEW method	Damping Overnead	Comment
SU(2)	Unitary		$\epsilon$	coherent	PEC	$1+4\epsilon$	
SU(2)	Unitary		$\epsilon$	coherent	Rescaling	$1+2\epsilon^2$	Slow WN convergence
SU(2)	Mixed Unitary		$\epsilon^2$	not Pauli	PEC	$1+4\epsilon^2$	Pauli frame unavailable
SU(2)	Mixed Unitary	✓	$\epsilon^2$	Pauli/depol	PEC	$1+4\epsilon^2$	
SU(2)	Mixed Unitary	✓	$\epsilon^2$	Pauli/depol	Rescaling	$1+2\epsilon^2$	
$R_z$	Unitary		$\epsilon$	coherent	PEC	$1+4\epsilon$	Pauli frame unavailable
$R_z$	Unitary		$\epsilon$	coherent	Rescaling	$1+2\epsilon^2$	Slow WN convergence
$R_z$	Mixed Unitary		$\epsilon^2$	not Pauli	PEC	$1+4\epsilon^2$	Pauli frame unavailable
$R_z$	Mixed Unitary	✓	$\epsilon^2$	Pauli/depol/XY	PEC	$1+4\epsilon^2$	
$R_z$	Mixed Unitary	✓	$\epsilon^2$	Pauli/depol/XY	ED + PEC	$1 + (q_x + q_y + 4q_z)\epsilon^2$	$q_z \sim \epsilon$ in numerics
$R_z$	Mixed Unitary	<b>√</b>	$\epsilon^2$	Pauli/depol/XY	ED + Resc.	$1 + (q_x + q_y + 2q_z)\epsilon^2$	$q_z \sim \epsilon$ in numerics
$R_z$	Mixed CPTP	<b>√</b>	$\epsilon^3$	Pauli Z	PEC	$1+4\epsilon^3$	Single ancilla
$R_z$	Mixed CPTP	✓	$\epsilon^3$	Pauli Z	Rescaling	$1+2\epsilon^3$	Single ancilla

TABLE II. Sampling overhead of error countermeasures under synthesis error of  $\epsilon$ . The remnant error indicates the diamond distance  $d(\mathcal{E}_{\text{rem}}, \mathcal{I})$  where  $\mathcal{I}$  is the identity channel. We assume that unitary gate synthesis is done with an accuracy of  $\epsilon$ , and compare the performance when we further perform mixed or error-crafted synthesis. The sampling overhead  $\gamma$  is indicated for a single gate, and the total overhead is multiplicative as  $\prod_{l} \gamma_{l}$  when overhead is  $\gamma_{l}$  for the l-th gate. The rescaling technique assumes that the underlying quantum circuit is sufficiently deep so that the white noise (WN) approximation holds [45, 54, 58]. We assume that the white noise approximation holds when the rescaling technique is applied. The cubic suppression in the last two rows is verified numerically up to  $\epsilon^{3} = 10^{-9}$  as shown in Fig. 5. Note that applying PEC for crafted and uncrafted synthesis differs significantly. We cannot rely on the Pauli frame in the latter, and an actual single-qubit operation is required.

for early FTQC circuits is of  $10^4$  for quantum dynamics simulation [30, 63] and  $10^6$  for ground state energy simulation [64], we envision that classical computation time is not bottleneck for such applications.

Last but not least, while we have exclusively discussed the error and sampling overhead only for the synthesis error, it must be kept in mind that, in reality, there is also incoherent noise that indirectly limits the synthesis accuracy. As can be seen from Fig. 5, one shall aim for the sweet spot where the total error is minimized. While we have displayed the case when we have designed the FTQC to contribute the majority of logical error to magic state distillation, we may flexibly change the scheme to introduce errors in Clifford operations as well.

#### DISCUSSION

In this work, we have proposed the scheme of error-crafted synthesis of single-qubit unitaries under the framework of Clifford+T formalism. We have proven that we can guarantee the quadratic suppression of the unitary synthesis error even when we constrain the remnant error to be Pauli and depolarizing channel. Furthermore, for the case of Pauli rotation gates, we have numerically shown that error crafting can yield biased Pauli noise such that sampling overhead to mitigate the errors can be suppressed quadratically compared to the existing techniques. We have also found that error crafting for CPTP maps that incorporate measurement and feedback operations achieves cubic suppression of the er-

ror up to accuracy of  $10^{-9}$ .

Numerous future directions are envisioned. First, it is essential to seek whether error crafting is possible for synthesis of multiqubit unitaries. Combined with the fact that the error can potentially be suppressed exponentially smaller with the qubit count for multiqubit case [41], it is crucial to extend the framework proposed in this work to perform practical quantum computation. Second, it is intriguing in terms of resource theoretic argument to assess the probabilistic transformability between channels. While this has been studied for state transformation in the context of magic state or entanglement distillation [65], the argument on quantum channels is left as an interesting open question. Third, it is an intriguing open question whether there is a lower bound on the computational complexity to perform error-crafted synthesis.

#### DATA AVAILABILITY

Data and codes for the work are available via GitHub repository [66].

#### ACKNOWLEDGEMENT

We thank fruitful discussions with Suguru Endo, Ali Javadi-Abhari, Yuuki Tokunaga, and Kunal Sharma. This work was supported by JST CREST Grant Number JPMJCR23I4, JST Moonshot R&D Grant Number JPMJCR23I4, Moonshot R&D Grant Number R&D Grant

ber JPMJMS2061, MEXT Q-LEAP Grant No. JPMXS0120319794, and No. JPMXS0118068682. N.Y. wishes to thank JST PRESTO No. JPMJPR2119, JST ERATO Grant Number JPMJER2302, JST Grant Number JPMJPF2221, and the support from IBM Quantum. S.A. is supported by JST, PRESTO Grant no.JPMJPR2111. This work is supported by MEXT Quantum Leap Flagship Program (MEXT Q-LEAP) Grant No. JP-MXS0118067394 and JPMXS0120319794, JST COI- NEXT Grant No. JPMJPF2014. K.T. is supported by World-leading Innovative Graduate Study Program for Materials Research, Information, and Technology (MERIT-WINGS) of the University of Tokyo and JSPS KAKENHI Grant No. JP24KJ0857.

#### **AUTHOR CONTRIBUTIONS**

N.Y. conceived the idea. N.Y., S.A., and K.T. performed theoretical analysis. N.Y. and H.M. developed the numerical codes. All authors contributed to scientific discussion and writing of the paper.

#### COMPETING INTERESTS

Y.S. and S.A. own stock/options in Nippon Telegraph and Telephone. Y.S. owns stock/options in QunaSys Inc.

- \* nyoshioka@ap.t.u-tokyo.ac.jp
- Peter W Shor, "Scheme for reducing decoherence in quantum computer memory," Phys. Rev. A 52, R2493 (1995).
- [2] Daniel Gottesman, "Stabilizer codes and quantum error correction," arXiv preprint quant-ph/9705052 (1997).
- [3] Peter W Shor, "Polynomial-time algorithms for prime factorization and discrete logarithms on a quantum computer," SIAM review 41, 303–332 (1999).
- [4] Daniel S. Abrams and Seth Lloyd, "Quantum algorithm providing exponential speed increase for finding eigenvalues and eigenvectors," Phys. Rev. Lett. 83, 5162–5165 (1999).
- [5] Alán Aspuru-Guzik, Anthony D Dutoi, Peter J Love, and Martin Head-Gordon, "Simulated quantum computation of molecular energies," Science 309, 1704–1707 (2005).
- [6] Jacob Biamonte, Peter Wittek, Nicola Pancotti, Patrick Rebentrost, Nathan Wiebe, and Seth Lloyd, "Quantum machine learning," Nature 549, 195 (2017).
- [7] Neereja Sundaresan, Theodore J. Yoder, Youngseok Kim, Muyuan Li, Edward H. Chen, Grace Harper, Ted Thorbeck, Andrew W. Cross, Antonio D. Córcoles, and Maika Takita, "Demonstrating multi-round subsystem quantum error correction using matching and maximum likelihood decoders," Nature Communications 14, 2852 (2023), publisher: Nature Publishing Group.
- [8] Laird Egan, Dripto M. Debroy, Crystal Noel, Andrew Risinger, Daiwei Zhu, Debopriyo Biswas, Michael Newman, Muyuan Li, Kenneth R. Brown, Marko Cetina, and Christopher Monroe, "Fault-tolerant control of an errorcorrected qubit," Nature 598, 281–286 (2021), publisher: Nature Publishing Group.
- [9] C. Ryan-Anderson, J. G. Bohnet, K. Lee, D. Gresh, A. Hankin, J. P. Gaebler, D. Francois, A. Chernoguzov, D. Lucchetti, N. C. Brown, T. M. Gatterman, S.K. Halit, K. Gilmore, J.A. Gerber, B. Neyenhuis, D. Hayes, and R.P. Stutz, "Realization of Real-Time Fault-Tolerant Quantum Error Correction," Physical Review X 11, 041058 (2021), publisher: American Physical Society.
- [10] Dolev Bluvstein, Simon J. Evered, Alexandra A. Geim, Sophie H. Li, Hengyun Zhou, Tom Manovitz, Sepehr Ebadi, Madelyn Cain, Marcin Kalinowski, Dominik Hangleiter, J. Pablo Bonilla Ataides, Nishad Maskara,

- Iris Cong, Xun Gao, Pedro Sales Rodriguez, Thomas Karolyshyn, Giulia Semeghini, Michael J. Gullans, Markus Greiner, Vladan Vuletić, and Mikhail D. Lukin, "Logical quantum processor based on reconfigurable atom arrays," Nature 626, 58–65 (2024), publisher: Nature Publishing Group.
- [11] William P. Livingston, Machiel S. Blok, Emmanuel Flurin, Justin Dressel, Andrew N. Jordan, and Irfan Siddiqi, "Experimental demonstration of continuous quantum error correction," Nature Communications 13, 2307 (2022), publisher: Nature Publishing Group.
- [12] K. J. Satzinger, Y. Liu, A. Smith, C. Knapp, M. Newman, C. Jones, Z. Chen, C. Quintana, X. Mi, A. Dunsworth, C. Gidney, I. Aleiner, F. Arute, K. Arya, J. Atalaya, R. Babbush, J. C. Bardin, R. Barends, J. Basso, A. Bengtsson, A. Bilmes, M. Broughton, B. B. Buckley, D. A. Buell, B. Burkett, N. Bushnell, B. Chiaro, R. Collins, W. Courtney, S. Demura, A. R. Derk, D. Eppens, C. Erickson, E. Farhi, L. Foaro, A. G. Fowler, B. Foxen, M. Giustina, A. Greene, J. A. Gross, M. P. Harrigan, S. D. Harrington, J. Hilton, S. Hong, T. Huang, W. J. Huggins, L. B. Ioffe, S. V. Isakov, E. Jeffrey, Z. Jiang, D. Kafri, K. Kechedzhi, T. Khattar, S. Kim, P. V. Klimov, A. N. Korotkov, F. Kostritsa, D. Landhuis, P. Laptev, A. Locharla, E. Lucero, O. Martin, J. R. McClean, M. McEwen, K. C. Miao, M. Mohseni, S. Montazeri, W. Mruczkiewicz, J. Mutus, O. Naaman, M. Neeley, C. Neill, M. Y. Niu, T. E. O'Brien, A. Opremcak, B. Pató, A. Petukhov, N. C. Rubin, D. Sank, V. Shvarts, D. Strain, M. Szalay, B. Villalonga, T. C. White, Z. Yao, P. Yeh, J. Yoo, A. Zalcman, H. Neven, S. Boixo, A. Megrant, Y. Chen, J. Kelly, V. Smelyanskiy, A. Kitaev, M. Knap, F. Pollmann, and P. Roushan, "Realizing topologically ordered states on a quantum processor," (2021).
- [13] Dolev Bluvstein, Harry Levine, Giulia Semeghini, Tout T. Wang, Sepehr Ebadi, Marcin Kalinowski, Alexander Keesling, Nishad Maskara, Hannes Pichler, Markus Greiner, Vladan Vuletić, and Mikhail D. Lukin, "A quantum processor based on coherent transport of entangled atom arrays," Nature 604, 451–456 (2022), publisher: Nature Publishing Group.
- [14] Youwei Zhao, Yangsen Ye, He-Liang Huang, Yiming Zhang, Dachao Wu, Huijie Guan, Qingling Zhu, Zuolin

- Wei, Tan He, Sirui Cao, Fusheng Chen, Tung-Hsun Chung, Hui Deng, Daojin Fan, Ming Gong, Cheng Guo, Shaojun Guo, Lianchen Han, Na Li, Shaowei Li, Yuan Li, Futian Liang, Jin Lin, Haoran Qian, Hao Rong, Hong Su, Lihua Sun, Shiyu Wang, Yulin Wu, Yu Xu, Chong Ying, Jiale Yu, Chen Zha, Kaili Zhang, Yong-Heng Huo, Chao-Yang Lu, Cheng-Zhi Peng, Xiaobo Zhu, and Jian-Wei Pan, "Realization of an Error-Correcting Surface Code with Superconducting Qubits," Physical Review Letters 129, 030501 (2022), publisher: American Physical Society.
- [15] Rajeev Acharya, Igor Aleiner, Richard Allen, Trond I. Andersen, Markus Ansmann, Frank Arute, Kunal Arya, Abraham Asfaw, Juan Atalaya, Ryan Babbush, Dave Bacon, Joseph C. Bardin, Joao Basso, Andreas Bengtsson, Sergio Boixo, Gina Bortoli, Alexandre Bourassa, Jenna Bovaird, Leon Brill, Michael Broughton, Bob B. Buckley, David A. Buell, Tim Burger, Brian Burkett, Nicholas Bushnell, Yu Chen, Zijun Chen, Ben Chiaro, Josh Cogan, Roberto Collins, Paul Conner, William Courtney, Alexander L. Crook, Ben Curtin, Dripto M. Debroy, Alexander Del Toro Barba, Sean Demura, Andrew Dunsworth, Daniel Eppens, Catherine Erickson, Lara Faoro, Edward Farhi, Reza Fatemi, Leslie Flores Burgos, Ebrahim Forati, Austin G. Fowler, Brooks Foxen, William Giang, Craig Gidney, Dar Gilboa, Marissa Giustina, Alejandro Grajales Dau, Jonathan A. Gross, Steve Habegger, Michael C. Hamilton, Matthew P. Harrigan, Sean D. Harrington, Oscar Higgott, Jeremy Hilton, Markus Hoffmann, Sabrina Hong, Trent Huang, Ashley Huff, William J. Huggins, Lev B. Ioffe, Sergei V. Isakov, Justin Iveland, Evan Jeffrey, Zhang Jiang, Cody Jones, Pavol Juhas, Dvir Kafri, Kostvantvn Kechedzhi, Julian Kelly, Tanui Khattar, Mostafa Khezri, Mária Kieferová, Seon Kim, Alexei Kitaev, Paul V. Klimov, Andrey R. Klots, Alexander N. Korotkov, Fedor Kostritsa, John Mark Kreikebaum, David Landhuis, Pavel Laptev, Kim-Ming Lau, Lily Laws, Joonho Lee, Kenny Lee, Brian J. Lester, Alexander Lill, Wayne Liu, Aditya Locharla, Erik Lucero, Fionn D. Malone, Jeffrey Marshall, Orion Martin, Jarrod R. McClean, Trevor McCourt, Matt McEwen, Anthony Megrant, Bernardo Meurer Costa, Xiao Mi, Kevin C. Miao, Masoud Mohseni, Shirin Montazeri, Alexis Morvan, Emily Mount, Wojciech Mruczkiewicz, Ofer Naaman, Matthew Neeley, Charles Neill, Ani Nersisyan, Hartmut Neven, Michael Newman, Jiun How Ng, Anthony Nguyen, Murray Nguyen, Murphy Yuezhen Niu, Thomas E. O'Brien, Alex Opremcak, John Platt, Andre Petukhov, Rebecca Potter, Leonid P. Pryadko, Chris Quintana, Pedram Roushan, Nicholas C. Rubin, Negar Saei, Daniel Sank, Kannan Sankaragomathi, Kevin J. Satzinger, Henry F. Schurkus, Christopher Schuster, Michael J. Shearn, Aaron Shorter, Vladimir Shvarts, Jindra Skruzny, Vadim Smelyanskiy, W. Clarke Smith, George Sterling, Doug Strain, Marco Szalay, Alfredo Torres, Guifre Vidal, Benjamin Villalonga, Catherine Vollgraff Heidweiller, Theodore White, Cheng Xing, Z. Jamie Yao, Ping Yeh, Juhwan Yoo, Grayson Young, Adam Zalcman, Yaxing Zhang, Ningfeng Zhu, and Google Quantum AI, "Suppressing quantum errors by scaling a surface code logical qubit," Nature 614, 676-681 (2023), publisher: Nature Publishing Group.

- [16] Kristan Temme, Sergey Bravyi, and Jay M. Gambetta, "Error mitigation for short-depth quantum circuits," Phys. Rev. Lett. 119, 180509 (2017).
- [17] Ying Li and Simon C. Benjamin, "Efficient variational quantum simulator incorporating active error minimization," Phys. Rev. X 7, 021050 (2017).
- [18] Suguru Endo, Simon C. Benjamin, and Ying Li, "Practical quantum error mitigation for near-future applications," Phys. Rev. X 8, 031027 (2018).
- [19] Bálint Koczor, "Exponential error suppression for nearterm quantum devices," Phys. Rev. X 11, 031057 (2021).
- [20] William J. Huggins, Sam McArdle, Thomas E. O'Brien, Joonho Lee, Nicholas C. Rubin, Sergio Boixo, K. Birgitta Whaley, Ryan Babbush, and Jarrod R. McClean, "Virtual distillation for quantum error mitigation," Phys. Rev. X 11, 041036 (2021).
- [21] Nobuyuki Yoshioka, Hideaki Hakoshima, Yuichiro Matsuzaki, Yuuki Tokunaga, Yasunari Suzuki, and Suguru Endo, "Generalized quantum subspace expansion," Phys. Rev. Lett. 129, 020502 (2022).
- [22] Ewout van den Berg, Zlatko K. Minev, and Kristan Temme, "Model-free readout-error mitigation for quantum expectation values," Phys. Rev. A 105, 032620 (2022).
- [23] Armands Strikis, Dayue Qin, Yanzhu Chen, Simon C. Benjamin, and Ying Li, "Learning-based quantum error mitigation," PRX Quantum 2, 040330 (2021).
- [24] Christophe Piveteau, David Sutter, Sergey Bravyi, Jay M. Gambetta, and Kristan Temme, "Error mitigation for universal gates on encoded qubits," Phys. Rev. Lett. 127, 200505 (2021).
- [25] Yasunari Suzuki, Suguru Endo, Keisuke Fujii, and Yuuki Tokunaga, "Quantum error mitigation as a universal error reduction technique: Applications from the nisq to the fault-tolerant quantum computing eras," PRX Quantum 3, 010345 (2022).
- [26] Nobuyuki Yoshioka, Tsuyoshi Okubo, Yasunari Suzuki, Yuki Koizumi, and Wataru Mizukami, "Hunting for quantum-classical crossover in condensed matter problems," npj Quantum Information 10, 45 (2024).
- [27] Ryan Babbush, Craig Gidney, Dominic W. Berry, Nathan Wiebe, Jarrod McClean, Alexandru Paler, Austin Fowler, and Hartmut Neven, "Encoding electronic spectra in quantum circuits with linear t complexity," Phys. Rev. X 8, 041015 (2018).
- [28] Joonho Lee, Dominic W. Berry, Craig Gidney, William J. Huggins, Jarrod R. McClean, Nathan Wiebe, and Ryan Babbush, "Even more efficient quantum computations of chemistry through tensor hypercontraction," PRX Quantum 2, 030305 (2021).
- [29] Kazuki Sakamoto, Hayata Morisaki, Junichi Haruna, Etsuko Itou, Keisuke Fujii, and Kosuke Mitarai, "End-to-end complexity for simulating the schwinger model on quantum computers," arXiv preprint arXiv:2311.17388 (2023).
- [30] Michael E Beverland, Prakash Murali, Matthias Troyer, Krysta M Svore, Torsten Hoefler, Vadym Kliuchnikov, Guang Hao Low, Mathias Soeken, Aarthi Sundaram, and Alexander Vaschillo, "Assessing requirements to scale to practical quantum advantage," arXiv preprint arXiv:2211.07629 (2022).
- [31] Bryan Eastin and Emanuel Knill, "Restrictions on transversal encoded quantum gate sets," Phys. Rev. Lett. **102**, 110502 (2009).

- [32] D. Aharonov, M. Ben-Or, R. Impagliazzo, and N. Nisan, "Limitations of Noisy Reversible Computation," (1996), arXiv:quant-ph/9611028.
- [33] Kento Tsubouchi, Takahiro Sagawa, and Nobuyuki Yoshioka, "Universal Cost Bound of Quantum Error Mitigation Based on Quantum Estimation Theory," Physical Review Letters 131, 210601 (2023), publisher: American Physical Society.
- [34] Ryuji Takagi, Hiroyasu Tajima, and Mile Gu, "Universal sampling lower bounds for quantum error mitigation," Phys. Rev. Lett. 131, 210602 (2023).
- [35] Yihui Quek, Daniel Stilck França, Sumeet Khatri, Johannes Jakob Meyer, and Jens Eisert, "Exponentially tighter bounds on limitations of quantum error mitigation," arXiv preprint arXiv:2210.11505 (2022).
- [36] Matthew B. Hastings, "Turning gate synthesis errors into incoherent errors," Quantum Info. Comput. 17, 488–494 (2017).
- [37] Earl Campbell, "Shorter gate sequences for quantum computing by mixing unitaries," Phys. Rev. A **95**, 042306 (2017).
- [38] Joel J Wallman and Joseph Emerson, "Noise tailoring for scalable quantum computation via randomized compiling," Physical Review A 94, 052325 (2016).
- [39] Vadym Kliuchnikov, Kristin Lauter, Romy Minko, Adam Paetznick, and Christophe Petit, "Shorter quantum circuits via single-qubit gate approximation," Quantum 7, 1208 (2023).
- [40] Seiseki Akibue, Go Kato, and Seiichiro Tani, "Probabilistic unitary synthesis with optimal accuracy," arXiv preprint arXiv:2301.06307 (2023).
- [41] Seiseki Akibue, Go Kato, and Seiichiro Tani, "Probabilistic state synthesis based on optimal convex approximation," npj Quantum Information 10, 1–9 (2024), publisher: Nature Publishing Group.
- [42] Jader P. Santos, Ben Bar, and Raam Uzdin, "Pseudo twirling mitigation of coherent errors in non-Clifford gates," npj Quantum Information 10, 100 (2024).
- [43] Tatsuki Odake, Philip Taranto, Nobuyuki Yoshioka, Toshinari Itoko, Kunal Sharma, Antonio Mezzacapo, and Mio Murao, "Robust error accumulation suppression," arXiv preprint arXiv:2401.16884 (2024).
- [44] Yosuke Mitsuhashi and Nobuyuki Yoshioka, "Clifford group and unitary designs under symmetry," PRX Quantum 4, 040331 (2023).
- [45] Kento Tsubouchi, Yosuke Mitsuhashi, Kunal Sharma, and Nobuyuki Yoshioka, "Symmetric clifford twirling for cost-optimal error mitigation in early fault-tolerant quantum computing," arXiv:2405.07720 (2024).
- [46] Neil J. Ross and Peter Selinger, "Optimal ancilla-free clifford+t approximation of z-rotations," Quantum Info. Comput. 16, 901–953 (2016).
- [47] Austin G. Fowler, "Constructing arbitrary steane code single logical qubit fault-tolerant gates," Quantum Info. Comput. 11, 867–873 (2011).
- [48] Alex Bocharov and Krysta M. Svore, "Resource-optimal single-qubit quantum circuits," Phys. Rev. Lett. 109, 190501 (2012).
- [49] Vadym Kliuchnikov, Dmitri Maslov, and Michele Mosca, "Fast and efficient exact synthesis of single-qubit unitaries generated by clifford and t gates," Quantum Info. Comput. 13, 607–630 (2013).
- [50] Alex Bocharov, Martin Roetteler, and Krysta M. Svore, "Efficient synthesis of universal repeat-until-

- success quantum circuits," Phys. Rev. Lett. 114, 080502 (2015).
- [51] Ewout van den Berg, Zlatko K. Minev, Abhinav Kandala, and Kristan Temme, "Probabilistic error cancellation with sparse Pauli–Lindblad models on noisy quantum processors," Nature Physics 19, 1116–1121 (2023), publisher: Nature Publishing Group.
- [52] Ryuji Takagi, "Optimal resource cost for error mitigation." Phys. Rev. Res. 3, 033178 (2021).
- [53] Frank Arute, Kunal Arya, Ryan Babbush, Dave Bacon, Joseph C. Bardin, Rami Barends, Rupak Biswas, Sergio Boixo, Fernando G. S. L. Brandao, David A. Buell, Brian Burkett, Yu Chen, Zijun Chen, Ben Chiaro, Roberto Collins, William Courtney, Andrew Dunsworth, Edward Farhi, Brooks Foxen, Austin Fowler, Craig Gidney, Marissa Giustina, Rob Graff, Keith Guerin, Steve Habegger, Matthew P. Harrigan, Michael J. Hartmann, Alan Ho, Markus Hoffmann, Trent Huang, Travis S. Humble, Sergei V. Isakov, Evan Jeffrey, Zhang Jiang, Dvir Kafri, Kostyantyn Kechedzhi, Julian Kelly, Paul V. Klimov, Sergey Knysh, Alexander Korotkov, Fedor Kostritsa, David Landhuis, Mike Lindmark, Erik Lucero, Dmitry Lyakh, Salvatore Mandrà, Jarrod R. McClean, Matthew McEwen, Anthony Megrant, Xiao Mi, Kristel Michielsen, Masoud Mohseni, Josh Mutus, Ofer Naaman, Matthew Neeley, Charles Neill, Murphy Yuezhen Niu, Eric Ostby, Andre Petukhov, John C. Platt, Chris Quintana, Eleanor G. Rieffel, Pedram Roushan, Nicholas C. Rubin, Daniel Sank, Kevin J. Satzinger, Vadim Smelyanskiy, Kevin J. Sung, Matthew D. Trevithick, Amit Vainsencher, Benjamin Villalonga, Theodore White, Z. Jamie Yao, Ping Yeh, Adam Zalcman, Hartmut Neven, and John M. Martinis, "Quantum supremacy using a programmable superconducting processor," Nature 574, 505-510 (2019).
- [54] Alexander M Dalzell, Nicholas Hunter-Jones, and Fernando GSL Brandão, "Random quantum circuits transform local noise into global white noise," Communications in Mathematical Physics 405, 78 (2024).
- [55] Hayata Morisaki, Seiseki Akibue, and Keisuke Fujii, "Optimal ancilla-free clifford+t compilation of single qubit unitary," in preparation (2024).
- [56] Bálint Koczor, "The dominant eigenvector of a noisy quantum state," New Journal of Physics 23, 123047 (2021).
- [57] Zhenyu Cai, Ryan Babbush, Simon C. Benjamin, Suguru Endo, William J. Huggins, Ying Li, Jarrod R. McClean, and Thomas E. O'Brien, "Quantum error mitigation," Rev. Mod. Phys. 95, 045005 (2023).
- [58] A. Morvan, B. Villalonga, X. Mi, S. Mandrà, A. Bengtsson, P. V. Klimov, Z. Chen, S. Hong, C. Erickson, I. K. Drozdov, J. Chau, G. Laun, R. Movassagh, A. Asfaw, L. T. A. N. Brandão, R. Peralta, D. Abanin, R. Acharya, R. Allen, T. I. Andersen, K. Anderson, M. Ansmann, F. Arute, K. Arya, J. Atalaya, J. C. Bardin, A. Bilmes, G. Bortoli, A. Bourassa, J. Bovaird, L. Brill, M. Broughton, B. B. Buckley, D. A. Buell, T. Burger, B. Burkett, N. Bushnell, J. Campero, H.-S. Chang, B. Chiaro, D. Chik, C. Chou, J. Cogan, R. Collins, P. Conner, W. Courtney, A. L. Crook, B. Curtin, D. M. Debroy, A. Del Toro Barba, S. Demura, A. Di Paolo, A. Dunsworth, L. Faoro, E. Farhi, R. Fatemi, V. S. Ferreira, L. Flores Burgos, E. Forati, A. G. Fowler, B. Foxen, G. Garcia, É. Genois, W. Giang,

C. Gidney, D. Gilboa, M. Giustina, R. Gosula, A. Grajales Dau, J. A. Gross, S. Habegger, M. C. Hamilton, M. Hansen, M. P. Harrigan, S. D. Harrington, P. Heu, M. R. Hoffmann, T. Huang, A. Huff, W. J. Huggins, L. B. Ioffe, S. V. Isakov, J. Iveland, E. Jeffrey, Z. Jiang, C. Jones, P. Juhas, D. Kafri, T. Khattar, M. Khezri, M. Kieferová, S. Kim, A. Kitaev, A. R. Klots, A. N. Korotkov, F. Kostritsa, J. M. Kreikebaum, D. Landhuis, P. Laptev, K.-M. Lau, L. Laws, J. Lee, K. W. Lee, Y. D. Lensky, B. J. Lester, A. T. Lill, W. Liu, W. P. Livingston, A. Locharla, F. D. Malone, O. Martin, S. Martin, J. R. McClean, M. McEwen, K. C. Miao, A. Mieszala, S. Montazeri, W. Mruczkiewicz, O. Naaman, M. Neeley, C. Neill, A. Nersisyan, M. Newman, J. H. Ng, A. Nguyen, M. Nguyen, M. Yuezhen Niu, T. E. O'Brien, S. Omonije, A. Opremcak, A. Petukhov, R. Potter, L. P. Pryadko, C. Quintana, D. M. Rhodes, C. Rocque, E. Rosenberg, N. C. Rubin, N. Saei, D. Sank, K. Sankaragomathi, K. J. Satzinger, H. F. Schurkus, C. Schuster, M. J. Shearn, A. Shorter, N. Shutty, V. Shvarts, V. Sivak, J. Skruzny, W. C. Smith, R. D. Somma, G. Sterling, D. Strain, M. Szalay, D. Thor, A. Torres, G. Vidal, C. Vollgraff Heidweiller, T. White, B. W. K. Woo, C. Xing, Z. J. Yao, P. Yeh, J. Yoo, G. Young, A. Zalcman, Y. Zhang, N. Zhu, N. Zobrist, E. G. Rieffel, R. Biswas, R. Babbush, D. Bacon, J. Hilton, E. Lucero, H. Neven, A. Megrant, J. Kelly, P. Roushan, I. Aleiner, V. Smelyanskiy, K. Kechedzhi, Y. Chen, and S. Boixo, "Phase transitions in random circuit sampling," Nature **634**, 328–333 (2024).

- [59] Aram W Harrow, Benjamin Recht, and Isaac L Chuang, "Efficient discrete approximations of quantum gates," Journal of Mathematical Physics 43, 4445–4451 (2002).
- [60] Ken Matsumoto and Kazuyuki Amano, "Representation of quantum circuits with clifford and  $\pi/8$  gates," arXiv preprint arXiv:0806.3834 (2008).
- [61] Jonas Haferkamp, Felipe Montealegre-Mora, Markus Heinrich, Jens Eisert, David Gross, and Ingo Roth, "Efficient unitary designs with a system-size independent number of non-clifford gates," Communications in Mathematical Physics 397, 995–1041 (2023).
- [62] Vadym Kliuchnikov, Dmitri Maslov, and Michele Mosca, "Practical approximation of single-qubit unitaries by single-qubit quantum clifford and t circuits," IEEE Transactions on Computers 65, 161–172 (2015).
- [63] Earl T Campbell, "Early fault-tolerant simulations of the hubbard model," Quantum Science and Technology 7, 015007 (2021).
- [64] Ian D Kivlichan, Craig Gidney, Dominic W Berry, Nathan Wiebe, Jarrod McClean, Wei Sun, Zhang Jiang, Nicholas Rubin, Austin Fowler, Alán Aspuru-Guzik, et al., "Improved fault-tolerant quantum simulation of condensed-phase correlated electrons via trotterization," Quantum 4, 296 (2020).
- [65] Bartosz Regula, "Probabilistic transformations of quantum resources," Phys. Rev. Lett. 128, 110505 (2022).
- [66] Nobuyuki Yoshioka, "error-crafting," GitHub Repository (2024).
- [67] John Watrous, "Semidefinite programs for completely bounded norms," arXiv preprint arXiv:0901.4709 (2009).
- [68] John Watrous, "Simpler semidefinite programs for completely bounded norms," arXiv preprint arXiv:1207.5726 (2012).
- [69] Abhinav Deshpande, Pradeep Niroula, Oles Shtanko, Alexey V. Gorshkov, Bill Fefferman, and Michael J. Gul-

lans, "Tight bounds on the convergence of noisy random circuits to the uniform distribution," PRX Quantum 3, 040329 (2022).

# Supplementary Notes for: Error Crafting in Mixed Quantum Gate Synthesis

#### CONTENTS

S1.	Limitation in applying twirling for non-Clifford operation	12
S2.	2. Formalism of mixed synthesis under diamond distance	13
	A. Simplification of mixed synthesis in single-qubit case	14
S3.	3. Numerical details on error crafting using unitaries	15
	A. Crafting Pauli channel	15
	B. Crafting depolarizing channel	15
	C. Crafting XY channel	16
S4.	4. Numerical details on error crafting using CPTP maps	17
S5.	5. Generation of shift unitaries with fixed diamond distance	18
S6.	6. White noise approximation under coherent errors	19
S7.	7. Theoretical guarantees for error crafted synthesis	21
	A. Crafting Pauli channel (Proof of Theorem 1)	21
	B. Crafting depolarizing channel	23
S8.	3. Technical lemmas	25
	A. Uniform continuity of $g_c(\epsilon,t)$	25
	B. Commutativity of lim and may for uniformly continuous functions	26

# S1. LIMITATION IN APPLYING TWIRLING FOR NON-CLIFFORD OPERATION

In the main text, we have explained using Table 1 that neither Pauli or Clifford twirling is not available for non-Clifford gates in general. Here we provide details on this argument.

Let  $\mathcal{U}$  denote a non-Clifford single-qubit gate and  $\mathcal{N}$  denote a noise channel associated to it. When we wish to realize the implementation of the target unitary with twirled noise, its channel representation can be written as

$$\mathbb{E}_{\mathcal{D}}[\mathcal{D}^{\dagger} \circ \mathcal{N} \circ \mathcal{D}] \circ \mathcal{U}, \tag{S1}$$

where  $\mathcal{D}$  is averaged over some single-qubit unitary subgroup such as the Pauli or Clifford group. However, a gate operation is always accompanied by the noise as  $\mathcal{N} \circ \mathcal{U}$ , and we cannot insert  $\mathcal{D}$  in between.

One of the options is to modify the expression as

$$\mathbb{E}_D[\mathcal{D}^{\dagger} \circ \mathcal{N} \circ \mathcal{U} \circ (\mathcal{U}^{\dagger} \circ \mathcal{D} \circ \mathcal{U})], \tag{S2}$$

which requires us to perform the following in sequence:

- (1) Operate conjugated unitary  $UDU^{\dagger}$  without noise.
- (2) Operate noisy target unitary.
- (3) Operate D without noise.

While the second and third steps are commonly considered to be achievable (coined as "hard" and "easy" operations in literature [38]), the problem is in the first step, since  $UDU^{\dagger}$  is a non-Clifford operation in general. For instance, if we consider  $U=e^{i\theta Z}$  and D=X, we must implement  $UDU^{\dagger}=e^{i\theta Z}Xe^{-i\theta Z}=e^{2i\theta Z}X$ . Since we assume that rotation gates are noisy, this cannot be implemented without injecting additional untwirled noise. This is however completely contrary to what we desire to do.

An exception is when the target gate belongs to the third level of the Clifford hierarchy. In this case,  $UDU^{\dagger}$  is a Clifford operation if D is a Pauli operator, and hence we can perform Pauli twirling by using Clifford gates. However, the Clifford twirling is not available; if we take the Hadamard gate, we can show that

$$(THT^{\dagger}) \cdot Z \cdot (THT^{\dagger})^{\dagger} = THZHT^{\dagger} = TXT^{\dagger} = SX. \tag{S3}$$

This indicates that  $THT^{\dagger}$  does not map a Pauli operator into a Pauli operator, and hence not a Clifford gate.

One might consider another style of twirling by implementing  $D^{\dagger}UD$  instead of  $UDU^{\dagger}$ . This direction is based on the fact that Eq. (S1) can also be formally rewritten as

$$\mathbb{E}_{\mathcal{D}}[\mathcal{D}^{\dagger} \circ \mathcal{N} \circ (\mathcal{D} \circ \mathcal{U} \circ \mathcal{D}^{\dagger}) \circ \mathcal{D}]. \tag{S4}$$

The requirement for this formulation is (1) the noise channel of  $D^{\dagger}UD$  is all identically  $\mathcal{N}$  irrespective of  $\mathcal{D}$  [38], and (2) the noise in  $\mathcal{D}$  is negligible. When the target is  $U = e^{i\theta P}$  with  $P \in \{X, Y, Z\}$  and  $\theta$  being the rotation angle, the requirement is that noise channel for Pauli rotation gates with angle  $\theta$  are identical to each other. However, this is unlikely in general, since the noise channel in unitary synthesis is unitary; to ensure the noise channel to be identical, we must accurately perform the unitary synthesis to control the synthesis error, which is beyond the actual task of synthesizing a target unitary up to accuracy of  $\epsilon$ .

#### S2. FORMALISM OF MIXED SYNTHESIS UNDER DIAMOND DISTANCE

In the main text, we have discussed the mixed synthesis that minimizes the diamond distance  $d_{\diamond}(\Phi_1, \Phi_2)$  between two unitary channels  $\Phi_1$  and  $\Phi_2$ . Here, we provide the formal definition of the diamond distance, which is related with the diamond norm as  $d_{\diamond}(\Phi_1, \Phi_2) := \frac{1}{2} \|\Phi_1 - \Phi_2\|_{\diamond}$  where  $\Phi_1, \Phi_2$  are linear maps from  $\mathcal{L}(\mathcal{H}_1)$  to  $\mathcal{L}(\mathcal{H}_2)$  (( $\mathcal{L}(\mathcal{H}_i)$ ): the entire set of linear map on  $\mathcal{H}_i$ ) for an d-dimensional Hilbert space  $\mathcal{H}(=\mathcal{H}_1=\mathcal{H}_2)$ :

$$\|\Phi_1 - \Phi_2\|_{\diamond} := \max_{\rho \in \mathbb{D}(\mathcal{H}_1 \otimes \mathcal{H}_2)} \|((\Phi_1 - \Phi_2) \otimes \mathrm{Id}_d)(\rho)\|_1.$$
 (S5)

Here,  $||X||_1 = \text{Tr}[\sqrt{X^{\dagger}X}]$  denotes the trace norm,  $\text{Id}_d$  is an identity channel acting on d-dimensional Hilbert space, and  $\mathbb{D}(\mathcal{H}_1 \otimes \mathcal{H}_2)$  is the set of physical density matrices on  $\mathcal{H}_1 \otimes \mathcal{H}_2$ . It is known that the diamond norm  $||\Phi||_{\diamond}$  can be efficiently calculated via semidefinite programming (SDP) for general linear maps as [67, 68]

$$\frac{\text{Primal problem}}{\text{maximize: } \frac{1}{2} \langle \mathcal{J}(\Phi), X \rangle + \frac{1}{2} \langle \mathcal{J}(\Phi)^{\dagger}, X^{\dagger} \rangle} \qquad \text{minimize: } \frac{1}{2} \| \text{Tr}_{\mathcal{H}_2} Y_0 \|_{\infty} + \frac{1}{2} \| \text{Tr}_{\mathcal{H}_2} Y_1 \|_{\infty} \\
\text{subject to: } \begin{pmatrix} \rho_0 \otimes \text{Id}_d & X \\ X^{\dagger} & \rho_1 \otimes \text{Id}_d \end{pmatrix} \geq 0, \qquad \text{subject to: } \begin{pmatrix} Y_0 & -\mathcal{J}(\Phi) \\ -\mathcal{J}(\Phi)^{\dagger} & Y_1 \end{pmatrix} \geq 0. \\
\rho_0, \rho_1 \in \mathbb{D}(\mathcal{H}_1), X \in \mathcal{L}(\mathcal{H}_1 \otimes \mathcal{H}_2). \qquad Y_0, Y_1 \in \mathcal{L}(\mathcal{H}_1) \otimes \mathcal{L}(\mathcal{H}_2), Y_0 = Y_0^{\dagger}, Y_1 = Y_1^{\dagger}. \\
\end{cases} (S6)$$

where  $\langle P,Q\rangle=\mathrm{Tr}[P^{\dagger}Q]$  is the inner product of operators P and  $Q,\,Y_0,Y_1\in\mathcal{L}(\mathcal{H}_1)\otimes\mathcal{L}(\mathcal{H}_2)$  are Hermitian matrices,  $\|\cdot\|_{\infty}$  is the spectral norm, and  $\mathcal{J}(\Phi)$  is the Choi operator of a map  $\Phi$  defined as  $\mathcal{J}(\Phi):=(\mathrm{Id}_d\otimes\Phi)[|\Omega\rangle\langle\Omega|]$  for the maximally entangled state  $|\Omega\rangle=\sum_i|i\rangle_{\mathcal{H}_1}|i\rangle_{\mathcal{H}_2}$ . By further assuming that  $\Phi_1$  and  $\Phi_2$  are completely positive and trace preserving (CPTP) maps, the calculation can be shown to be simplified as follows.

Now let us consider mixed synthesis of a target CPTP map  $\hat{\Upsilon}$  using a set of CPTP implementable maps  $\{\Upsilon_j\}$  under the following minimization problem:

minimize: 
$$\frac{1}{2} \left\| \hat{\Upsilon} - \sum_{j} p_{j} \Upsilon_{j} \right\|_{\diamond}$$
 subject to:  $p_{j} \geq 0, \sum_{j} p_{j} = 1$ . (S8)

While it seems complicated since the diamond norm is already defined by minimization, it can be shown that we can solve Eq. (S8) via SDP:

**Proposition 1.** Let  $\hat{\Upsilon}$  and  $\{\Upsilon_j\}$  be a target CPTP map and a finite set of implementable CPTP maps from  $\mathcal{L}(\mathcal{H}_1)$  to  $\mathcal{L}(\mathcal{H}_2)$ , respectively. Then, the distance  $\min_{p = \frac{1}{2}} \|\hat{\Upsilon} - \sum_j p_j \Upsilon_j\|_{\diamond}$  and the optimal probability distribution  $\{p_j\}$  can be computed with the following SDP:

$$\frac{\text{Primal problem}}{\text{maximize: } \text{Tr}[\mathcal{J}(\hat{\Upsilon})T] - t} \qquad \qquad \frac{\text{Dual problem}}{\text{minimize: } w \in \mathbb{R}} \\
\text{subject to: } 0 \leq T \leq \rho \otimes \text{Id}_{\mathcal{H}_2}, \qquad \qquad \text{subject to: } S \geq 0, S \geq \mathcal{J}\left(\hat{\Upsilon} - \sum_{j} p_j \Upsilon_j\right), \qquad (S9) \\
\rho \in \mathcal{D}(\mathcal{H}_1), \qquad \qquad w \text{Id}_{\mathcal{H}_1} \geq \text{Tr}_{\mathcal{H}_2}[S], \\
\forall j, \text{Tr}[\mathcal{J}(\Upsilon_j)T] \leq t. \qquad \forall p_j \geq 0, \sum_{j} p_j \leq 1.$$

Note that the strong duality holds in this SDP, i.e., the optimum primal and dual values are equal.

#### A. Simplification of mixed synthesis in single-qubit case

Although SDP is efficient in a sense that there exists a polynomial-time algorithm with respect to the problem matrix size, in practice the runtime grows quite rapidly, and hence it is desirable to simplify the minimization problem. For the single-qubit case, the calculation of diamond distance boils down to that of trace distance between Choi matrices. While one can show  $\frac{1}{d}\|\Phi_1 - \Phi_2\|_{\diamond} \leq \frac{1}{d}\|\mathcal{J}(\Phi_1) - \mathcal{J}(\Phi_2)\|_1 \leq \|\Phi_1 - \Phi_2\|_{\diamond}$  for general d-dimensional completely positive maps  $\Phi_1$  and  $\Phi_2$ , for the single-qubit mixed unitary channel case it is known to saturate the lower bound as  $\|\Phi_1 - \Phi_2\|_{\diamond} = \|\mathcal{J}(\Phi_1) - \mathcal{J}(\Phi_2)\|_1/2$ . Therefore, the remnant error of mixed synthesis,  $\min_p \frac{1}{2} \|\hat{\Upsilon} - \sum_j p_j \Upsilon_j\|_{\diamond}$ , can now be computed by the following simpler semidefinite programming problem:

We further find that it is convenient to introduce the notion of magic basis, an orthonormal basis for the Choi representation of single-qubit channels:

$$|\Psi_{1}\rangle = \frac{1}{\sqrt{2}}(|00\rangle + |11\rangle), \qquad |\Psi_{2}\rangle = \frac{i}{\sqrt{2}}(|00\rangle - |11\rangle),$$
  
$$|\Psi_{3}\rangle = \frac{i}{\sqrt{2}}(|01\rangle + |10\rangle), \qquad |\Psi_{4}\rangle = \frac{1}{\sqrt{2}}(|01\rangle - |10\rangle). \tag{S11}$$

It can be shown that this relates a single-qubit unitary channel  $\mathcal{U}$  to a unit vector  $r = (r_1, r_2, r_3, r_4)^T \in \mathbb{R}^4$  as follows,

$$\frac{1}{2} \left[ \mathcal{J}(\mathcal{U}) \right]_{MB} = rr^T, \tag{S12}$$

where  $([\cdot]_{MB})_{ij} = \langle \Psi_i | \cdot | \Psi_j \rangle$ .

When we explicitly consider the distance between a target unitary  $\hat{\mathcal{U}}$  and a mixture of unitaries  $\sum_{j} p_{j}\mathcal{U}_{j}$ , we can rewrite the expression of the diamond distance as

$$d_{\diamond}\left(\hat{\mathcal{U}}, \sum_{j} p_{j} \mathcal{U}_{j}\right) = \frac{1}{2} \left\|\hat{\mathcal{U}} - \sum_{j} p_{j} \mathcal{U}_{j}\right\|_{\diamond} = \frac{1}{2} \cdot \frac{1}{2} \left\|\mathcal{J}(\mathcal{U}) - \sum_{j} p_{j} \mathcal{J}(\mathcal{U}_{j})\right\|_{1} = \frac{1}{2} \left\|rr^{T} - \sum_{j} p_{j} r^{(j)} r^{(j)T}\right\|_{1}, \quad (S13)$$

where r and  $r^{(j)}$  are the unit vectors obtained from the magic basis representation of  $\hat{\mathcal{U}}$  and  $\mathcal{U}_j$ , respectively. Furthermore, since the trace norm  $||A||_1$  is simply a sum of diagonal elements when A is diagonal, the diamond distance can be simplified when  $\hat{\mathcal{U}}$  is identity and  $\sum_j p_j \mathcal{U}_j$  is a single-qubit Pauli channel as

$$d_{\diamond}\left(\hat{\mathcal{U}}, \sum_{j} p_{j} \mathcal{U}_{j}\right) = \frac{1}{2}\left(\left(1 - \sum_{j} p_{j}(r_{1}^{(j)})^{2}\right) + \sum_{k=2}^{4} \sum_{j} p_{j}(r_{k}^{(j)})^{2}\right) = 1 - \sum_{j} p_{j}(r_{1}^{(j)})^{2},\tag{S14}$$

where we have used  $\sum_{k=2}^{4} (r_k^{(j)})^2 = 1 - (r_1^{(j)})^2$  for the second equation. As we discuss in Sec. S3, this simplification is beneficial since the minimization problem of the diamond distance can be formulated by linear programming problem instead of the cumbersome SDP.

#### S3. NUMERICAL DETAILS ON ERROR CRAFTING USING UNITARIES

#### A. Crafting Pauli channel

As discussed in the main text, the minimization problem regarding the error-crafted synthesis of a Pauli channel is formulated via the following constrained minimization problem of a probability distribution  $\{p_j\}$  given a target unitary channel  $\hat{\mathcal{U}}$  and a set of synthesized unitaries  $\{\mathcal{U}_j\}$  as follows:

minimize 
$$\frac{1}{2} \left\| \hat{\mathcal{U}} - \sum_{j} p_{j} \mathcal{U}_{j} \right\|_{\diamond}$$
 subject to  $\sum_{j} p_{j} \mathcal{U}_{j} \circ \hat{\mathcal{U}}^{-1}(\cdot) = \sum_{a} \chi_{aa} P_{a} \cdot P_{a}, \chi_{aa} \ge 0,$  (S15)

where  $P_a \in \{I, X, Y, Z\}$  is a single-qubit Pauli operator. In a practical sense, an equality constraint tends to yield numerical instability, and therefore we relax the condition for the remnant error  $\mathcal{E}_{rem} = (\sum_j p_j \mathcal{U}_j) \circ \hat{\mathcal{U}}^{-1}$  to allow a small violation as

minimize 
$$\frac{1}{2} \left\| \hat{\mathcal{U}} - \sum_{j} p_{j} \mathcal{U}_{j} \right\|_{\hat{\Omega}}$$
 subject to  $\sum_{j} p_{j} \mathcal{U}_{j} \circ \hat{\mathcal{U}}^{-1}(\cdot) = \sum_{ab} \chi_{ab} P_{a} \cdot P_{b}, \sum_{a \neq b} |\chi_{ab}| \leq g_{1},$  (S16)

where  $g_1$  is a tolerance factor regarding the Pauli error constraint.

When the set  $\{\mathcal{U}_j\}$  is not appropriately generated, there does not exist any feasible solution for Eq. (S15). While numerical solvers such as Gurobi offer an automated way to relax the equation constraint, via the variable presolve, we find that this precomputation is done too aggressively so that the accuracy of the minimization is quite poor. Instead, in our work, we have done a logarithmic search of  $g_1$ , starting from machine precision of  $g_1 = 10^{-16}$ . We have defined the error crafting to be successful if we find feasible solution such that (1)  $\min \frac{1}{2} \|\hat{\mathcal{U}} - \sum_j p_j \mathcal{U}_j\|_{\diamond} \leq (c+1)^2 \epsilon^2$ , and (2)  $g_1 \leq 10^{-12}$  are both satisfied.

As we discussed in Sec. S2, the minimization problem boils down to a linear programming problem under the magic basis. The minimization problem equivalent to Eq. (S15) is

minimize 
$$1 - \sum_{j} p_j \left(r_1^{(j)}\right)^2$$
 subject to  $\sum_{j} p_j = 1, p_j \ge 0, \sum_{j} p_j r^{(j)} r^{(j)T}$  is diagonal, (S17)

where  $r^{(j)} = (r_1^{(j)}, r_2^{(j)}, r_3^{(j)}, r_4^{(j)})^T \in \mathbb{R}^4$  corresponds to the magic basis representation of  $\mathcal{U}_j \circ \hat{\mathcal{U}}^{-1}$ . After relaxing the equality constraint, the minimization problem is given as

minimize 
$$1 - \sum_{j} p_j \left( r_1^{(j)} \right)^2$$
 subject to  $\sum_{j} p_j = 1, p_j \ge 0, \sum_{k \ne k'} \left| \sum_{j} p_j r_k^{(j)} r_{k'}^{(j)} \right| \le g_1',$  (S18)

where  $g'_1$  is the tolerance factor in this representation. We find that accuracy is much enhanced when the minimization (and relaxation) is done under this representation. In practice, we solve Eq. (S18) using LP implemented in Gurobi or SciPy, and check if the conditions are satisfied.

### B. Crafting depolarizing channel

Here, we provide numerical details regarding the error crafting of depolarizing channels. In similar to Sec. S3 A, the minimization problem is defined as

minimize 
$$\frac{1}{2} \left\| \hat{\mathcal{U}} - \sum_{j} p_{j} \mathcal{U}_{j} \right\|_{\hat{\Omega}}$$
 subject to  $\sum_{a} \chi_{aa} = 1, \chi_{XX} = \chi_{YY} = \chi_{ZZ} \ge 0, \chi_{a \ne b} = 0,$  (S19)

where the set of shift unitary  $\{\mathcal{V}_{j}^{(c\epsilon)}\}_{j=1}^{9}$  consists of nine elements, in contrast to seven for the Pauli constraint. Again we relax the equality constraints into inequality constraints for the sake of numerical stability. Concretely, we solve the following problem:

minimize 
$$\frac{1}{2} \left\| \hat{\mathcal{U}} - \sum_{j} p_{j} \mathcal{U}_{j} \right\|_{\diamond}$$
 subject to  $\sum_{a} \chi_{aa} = 1, \max_{a' \neq b'} \{ |\chi_{a'a'} - \chi_{b'b'}| \} \le g_{2}, \sum_{a \neq b} |\chi_{ab}| \le g_{1},$  (S20)

where  $a \in \{I, X, Y, Z\}$  and  $a', b' \in \{X, Y, Z\}$ . We regard the error crafting to be successful if (1) min  $\frac{1}{2} \|\hat{\mathcal{U}} - \sum_{j} p_{j} \mathcal{U}_{j}\|_{\diamond} \le (c+1)^{2} \epsilon^{2}$ , (2)  $g_{1} \le 10^{-12}$ , and (3)  $g_{2} \le 0.01(\sum_{a' \in \{X,Y,Z\}} \chi_{a'a'}) \sim 0.01 \epsilon^{2}$  are all satisfied. For completeness, we mention that the minimization problem can also be expressed in the magic basis representation as

minimize 
$$1 - \sum_{j} p_j \left( r_1^{(j)} \right)^2$$
 subject to  $\sum_{j} p_j = 1, p_j \ge 0, \sum_{j} p_j r^{(j)} r^{(j)T} = (1 - q) \mathbf{e}^{(1)} \mathbf{e}^{(1)T} + \frac{q}{4} \mathrm{Id},$  (S21)

where  $\mathbf{e}^{(i)}$  is a vector whose element is 0 except the *i*th element. After relaxing the equality into inequality, we now have

minimize 
$$1 - \sum_{j} p_{j} \left(r_{1}^{(j)}\right)^{2}$$
subject to  $\sum_{j} p_{j} = 1, p_{j} \geq 0, \quad \max_{k \neq k'} \left\{ \left| \sum_{j} p_{j} \left(r_{k}^{(j)} r_{k}^{(j)} - r_{k'}^{(j)} r_{k'}^{(j)}\right) \right| \right\} \leq g_{2}', \quad \sum_{k \neq k'} \left| \sum_{j} p_{j} r_{k}^{(j)} r_{k'}^{(j)} \right| \leq g_{1}', \quad (S22)$ 

where  $g'_2$  is the tolerance factor for the homogeneity of the Pauli error rates.

The results of error-crafted synthesis are shown in Fig. S1. We observe the validity of the nine-shift unitary from the bounded behavior in Fig. S1(a). As in the case of the Pauli constraint, we also observe a boost in the accuracy by expanding the size of the basis set by a factor of R. From Figs. S1(b), (c), and (d), we further find that both increasing c and R contribute to the suppression of the failure probability of the error crafting.

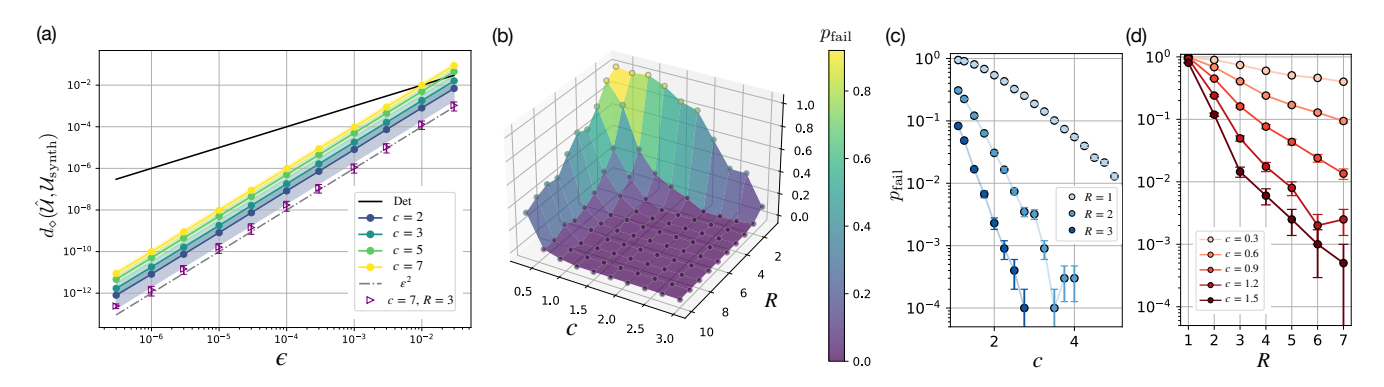


FIG. S1. (a) Diamond distance  $d_{\circ}(\hat{\mathcal{U}}, \mathcal{U}_{\mathrm{synth}})$  between the target single-qubit Haar random unitary  $\hat{\mathcal{U}}$  and synthesized channel  $\mathcal{U}_{\mathrm{synth}} := \sum_{j} p_{j}\mathcal{U}_{j}$ , with the remnant error constrained to the single-qubit depolarizing channel. The black real line indicates the results from unitary synthesis by the Ross-Selinger algorithm [46], while the filled dots are results from error-crafted synthesis with shift factors of c=2,3,5,7. When we expand the basis set size by a factor of R=3, shown by unfilled triangles, the effective synthesis error is suppressed below the bound in Eq. (862) and approaches the value of  $\epsilon^{2}$ . The shown data are mean over 200 random instances of target unitaries. (b) Failure rate of error-crafted synthesis, averaged over 50 instances. (c)(d) Suppression of  $p_{\mathrm{fail}}$  with shift factor c and R. The data is averaged over 10000 and 2000 instances, respectively.

#### C. Crafting XY channel

We finally describe the minimization problem to craft XY channels. Namely, we wish to solve the following:

minimize 
$$\frac{1}{2} \left\| \hat{\mathcal{U}} - \sum_{j} p_{j} \mathcal{U}_{j} \right\|_{\diamond}$$
 subject to  $\chi_{XX} + \chi_{YY} = 1, \chi_{ZZ} = 0, \chi_{a \neq b} = 0,$  (S23)

where the set of shift unitary  $\{\mathcal{V}_{j}^{(c\epsilon)}\}$  is generated according to the procedure shown in Sec. S5. To enhance the numerical stability, we have relaxed the equality constraint for  $\chi_{ZZ}$  into inequality as

minimize 
$$\frac{1}{2} \left\| \hat{\mathcal{U}} - \sum_{j} p_{j} \mathcal{U}_{j} \right\|_{\hat{\Omega}}$$
 subject to  $\sum_{a} \chi_{a} = 1, \max_{a' \neq b'} \{ |\chi_{ZZ}| \} \le g_{2}, \sum_{a \neq b} |\chi_{a \neq b}| \le g_{1},$  (S24)

where tolerance factors  $g_1$  and  $g_2$  are chosen in similar to those for depolarizing channels. Using the magic basis, the minimization problem is expressed as

minimize 
$$1 - \sum_{j} p_{j} \left(r_{1}^{(j)}\right)^{2}$$
  
subject to  $\sum_{j} p_{j} = 1, p_{j} \geq 0, \sum_{j} p_{j} r_{2}^{(j)} r_{2}^{(j)} = 0, \sum_{j} p_{j} r^{(j)} r^{(j)T}$  is diagonal, (S25)

and after the relaxation of the equality constraint into inequality we have

minimize 
$$1 - \sum_{j} p_{j} \left(r_{1}^{(j)}\right)^{2}$$
  
subject to  $\sum_{j} p_{j} = 1, p_{j} \geq 0, \quad \left|\sum_{j} p_{j} r_{2}^{(j)} r_{2}^{(j)}\right| \leq g'_{2}, \quad \sum_{k \neq k'} \left|\sum_{j} p_{j} r_{k}^{(j)} r_{k'}^{(j)}\right| \leq g'_{1},$  (S26)

where  $g'_2$  is the tolerance factor for suppressing the Z component of the Pauli channel and  $g'_1$  is for non-unital components.

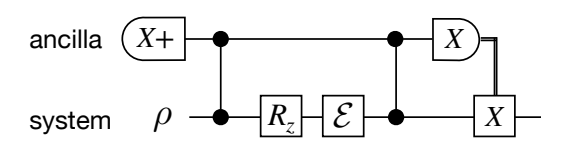


FIG. S2. Measurement and feedback protocol that corrects X error in implementing a Pauli Z rotation.

#### S4. NUMERICAL DETAILS ON ERROR CRAFTING USING CPTP MAPS

As discussed in the main text, the error of Pauli rotation can be suppressed significantly by applying the error crafting for CPTP maps that represents the channel of synthesized gates accompanied by error correction circuit as shown in Fig. S2. In similar to the cases in Sec. S3, the minimization problem is defined as

$$\frac{1}{2} \left\| \hat{\mathcal{U}} - \sum_{j} p_{j} \Lambda_{j} \right\|_{\diamond} \quad \text{subject to} \quad \sum_{j} p_{j} \Lambda_{j} \circ \hat{\mathcal{U}}^{-1}(\cdot) = \sum_{a} \chi_{aa} P_{a} \cdot P_{a}, \chi_{aa} \ge 0, \tag{S27}$$

where  $\{\Lambda_j\}$  is the set of implementable CPTP maps. Concretely for the case of Pauli rotation, with the target unitary and synthesized unitary channels expressed as  $\hat{\mathcal{U}}$  and  $\mathcal{U}_j$ , respectively, we can express the effective CPTP map  $\Lambda_j$  and remnant error  $\mathcal{E}_{\text{rem},j}$  obtained from logical error correction as

$$\Lambda_{j} = \mathscr{T}\left(\mathcal{C} \circ \mathcal{M}_{X}^{(A)} \circ \mathcal{W}_{E}' \circ \mathcal{U}_{j} \circ \mathcal{W}_{E} \circ (\Pi_{X+}^{(A)})\right), \tag{S28}$$

$$\mathcal{E}_{\text{rem},j} = \mathscr{T}\left(\mathcal{C} \circ \mathcal{M}_X^{(A)} \circ \mathcal{W}_E' \circ (\mathcal{U}_j \circ \hat{\mathcal{U}}^{-1}) \circ \mathcal{W}_E \circ (\Pi_{X+}^{(A)})\right), \tag{S29}$$

where  $\mathscr{T}$  trace outs the ancillary qubit,  $\mathscr{C}$  is the correction operation conditioned by the result of the X-measurement on ancilla  $\mathscr{M}_{X}^{(A)}$ ,  $\mathscr{W}_{E}$ ,  $\mathscr{W}_{E}'$  is the entangling operation between the target and ancilla qubit, and  $\Pi_{X+}^{(A)}$  is the state

preparation (or force initialization) of  $|+\rangle$  state on the ancilla. Note that the expression of Eq. (S29) follows from the fact that  $W_E$  and  $W_E'$  commutes with the target unitary  $\hat{\mathcal{U}}$ .

Without loss of generality, we consider the single-qubit Pauli Z rotation in the following. First, note that, for the case of Pauli rotations, the goal of finding an appropriate set of CPTP maps and their weights  $\{(p_j, \Lambda_j)\}_j$  is equivalent to finding an appropriate set of  $\{p_j, \mathcal{E}_{\text{rem},j}\}_j$ . It is straightforward to see that the Pauli transfer matrix of a remnant error channel  $\mathcal{E}_{\text{rem},j}$  for a Pauli Z rotation, denoted as  $\Gamma_{\mathcal{E}_{\text{rem},j}}$ , can be expressed as

$$\Gamma_{\mathcal{E}_{\text{rem},j}} = \begin{pmatrix}
1 & 0 & 0 & 0 \\
0 & 1 - \mu_j & \nu_j & 0 \\
0 & -\nu_j & 1 - \mu_j & 0 \\
0 & 0 & 0 & 1
\end{pmatrix},$$
(S30)

where  $0 \le \mu_j \le 1$  and  $\Gamma_{\mathcal{E}_{\text{rem},j}} \ge 0$ . This motivates us to find a pair of remnant error channels  $\mathcal{E}_{\text{rem},+}$  and  $\mathcal{E}_{\text{rem},-}$  which satisfies (i)  $\nu_+ > 0$ ,  $\nu_- < 0$ , (ii)  $\mu_{\pm} = O(\epsilon^3)$ , which follows from the geometric interpretation described in the main text. Once such a pair is found, we take the mixture of them as

$$\tilde{\mathcal{E}}_{\text{rem}} = \frac{\nu_{-}}{\nu_{+} + \nu_{-}} \mathcal{E}_{\text{rem},+} + \frac{\nu_{+}}{\nu_{+} + \nu_{-}} \mathcal{E}_{\text{rem},-},$$
(S31)

$$\Gamma_{\tilde{\mathcal{E}}_{\text{rem}}} = \begin{pmatrix} 1 & 0 & 0 & 0 \\ 0 & 1 - \tilde{\mu} & 0 & 0 \\ 0 & 0 & 1 - \tilde{\mu} & 0 \\ 0 & 0 & 0 & 1 \end{pmatrix}, \tag{S32}$$

which is a purely Z error channel with an error rate of  $\tilde{\mu} = \frac{\nu_-}{\nu_+ + \nu_-} \mu_+ + \frac{\nu_+}{\nu_+ + \nu_-} \mu_- = O(\epsilon^3)$ .

We note that the current search algorithm is based on a brute-force search, and hence the computational complexity is expected to scale as  $O(K/\epsilon)$  where K is the number of shift unitaries. We leave an open question of whether there is any bound on complexity to search the pair as in the above discussion. In the current implementation, we generate around 3000 unitaries to reach a remnant error of  $10^{-6}$  and around 20000 unitaries to reach  $10^{-9}$ , with each unitary synthesis done in milliseconds using a direct search algorithm proposed in Ref. [55]. Note that each unitary synthesis is independent, and hence is embarrassingly parallelizable.

#### S5. GENERATION OF SHIFT UNITARIES WITH FIXED DIAMOND DISTANCE

In this section, we discuss how to generate a set of S shift unitaries  $\{\mathcal{V}_s^{\epsilon}\}_{s=1}^{S}$  which all satisfies  $d_{\diamond}(\mathcal{V}_s^{\epsilon}, \mathcal{I}) = \epsilon$ . One of such a method is to generate Haar random unitaries and constrain the "rotation angle" by noting that any single-qubit unitary can be written as  $e^{i\theta \sum_{a=X,Y,Z} n_a P_a}$  where  $(n_X, n_Y, n_Z)^T \in \mathbb{R}^3$  is a unit vector. However, we have found that such a protocol is unsatisfactory in terms of efficiency in generating independent unitaries after unitary synthesis. Therefore, we instead utilize the magic basis representation of a single-qubit unitary. To be precise, given a unit vector  $\tilde{v} \in \mathbb{R}^3$ , we can generate a single-qubit unitary that is expressed in the magic basis representation as

$$ee^T = \frac{1}{2} \left[ \mathcal{J}(\mathcal{U}) \right]_{MB} \text{ with } e = \begin{pmatrix} \sqrt{1 - \epsilon^2} \\ \epsilon \tilde{v} \end{pmatrix}.$$
 (S33)

Therefore, we may generate unit vectors in order to generate a set of shift unitaries with a fixed value of the diamond distance as follows:

- Step 1. Generate a set of unit vectors  $\{\tilde{v}_s|\tilde{v}_s \in \mathbb{R}^3, \|\tilde{v}_s\|_2 = 1\}_{s=1}^S$  so that the vectors are distributed on the surface of the sphere as homogeneously as possible.
- Step 2. Compute the Choi matrix in the magic basis representation,  $\{[\mathcal{J}(\mathcal{V}_s^{(\epsilon)})]_{MB}\}$ , using the relationship (S33).
- Step 3. Perform basis transformation to obtain  $\{\mathcal{J}(\mathcal{V}_s^{\epsilon})\}$  in the computational basis, and then compute the matrix representation of shift unitaries  $\{V_s^{\epsilon}\}$ .

In practice, we have employed numerical optimization for Step 1.

TABLE S1. Performance of the QEM through rescaling the noisy expectation value assuming the white-noise approximation for incoherent error with error rate p and coherent error with diamond norm  $\epsilon_{\text{coh}}^2$ . While coherent errors have quadratically suppressed sampling overhead, their effect on the bias is comparable with incoherent errors.

Error model	Bias	Sampling overhead
Incoherent error		$(1+O(p))^{2nL}$
Coherent error	$O(\sqrt{nL}\epsilon_{\mathrm{coh}})$	$(1 + O(\epsilon_{\rm coh}^2))^{2nL}$

#### WHITE NOISE APPROXIMATION UNDER COHERENT ERRORS

The white noise, or equivalently the global depolarizing noise on d-dimensional system acting as  $\mathcal{E}_{wn}(\cdot) = (1-p)$ .  $+p\mathrm{Id}/d$  under the rate p, is one of the most desirable error profile in the context of estimating expectation values of physical observables. The main reasons are two-fold:  $\mathcal{E}_{wn}$  commutes with any gate operations, and it allows unbiased estimation with optimal sampling overhead. All the expectation values of traceless observables shrink homogeneously by a factor of 1-p under a single application of  $\mathcal{E}_{wn}$ , and hence we can unbiasedly estimate the expectation value of an observable O from a noisy estimation as  $\langle O \rangle = (1-p)^{-1} \langle O \rangle_{\text{noisy}}$ . In the case when we have L applications of  $\mathcal{E}_{wn}$ , we can simply replace  $(1-p)^{-1}$  with  $(1-p)^{-L}$  and mitigate error with minimal sampling overhead of  $(1-p)^{-2L}$ .

The white noise has been argued to be realized in experiments, in particular when the unitary gates are chosen at random [53]. In fact, one can prove that, even if the qubit connectivity is only linear and the circuit constitutes a brick-wall structure with random Haar unitary gates for two qubits, the effective noise converges to the white noise under unital noise [54, 69]. However, these arguments mainly consider incoherent error, and how coherent error can affect the white-noise approximation is not fully examined. Given that the synthesis error is inevitable in the early FTQC regime, it is crucial to investigate the effect of coherent errors on the white-noise approximation.

Let us assume that one aims to simulate a n-qubit layered quantum circuit  $\hat{\mathcal{U}} := \mathcal{U}_{L+1} \circ \mathcal{U}_L \circ \cdots \circ \mathcal{U}_1$  which is exposed to noise channels as  $\mathcal{U} = \mathcal{U}_{L+1} \circ \mathcal{E} \circ \mathcal{U}_L \circ \cdots \mathcal{E} \circ \mathcal{U}_1$ . We define the effective noise channel  $\mathcal{E}'$  by re-expressing the noisy layered circuit as  $\mathcal{U} = \mathcal{E}' \circ \hat{\mathcal{U}}$ , When we expect that  $\mathcal{E}'$  is close to the global white noise, we can mitigate errors and restore the ideal expectation value via some constant factor R, namely by rescaling the noisy one as  $\operatorname{tr}[\rho O] = R\operatorname{tr}[\mathcal{E}'(\rho)O]$ . Especially when each unitary layer  $\mathcal{U}_l(\cdot) = U_l \cdot U_l^{\dagger}$  is chosen randomly from n-qubit Haar random unitary, we can bound the bias between the ideal and the rescaled expectation value as

$$\mathbb{E}_{U}\left[\left|R\mathrm{tr}[\mathcal{E}'(\rho)O] - \mathrm{tr}[\rho O]\right|\right] \le \sqrt{1 - \left(\frac{s^{2}}{u}\right)^{L}},\tag{S34}$$

by choosing the rescaling factor as  $R = (s/u)^L$  (Theorem S2 of [45]). Here, u and s are noise-dependent constants called *unitarity* and *average noise strength*, respectively, which can be represented as

$$u = \frac{\sum_{ij} |\text{tr}[E_i E_j^{\dagger}]|^2 - 1}{4^n - 1}$$
 (S35)

$$s = \frac{\sum_{i} |\text{tr}[E_i]|^2 - 1}{4^n - 1},$$
 (S36)

where  $E_i$  is the Kraus operators of the noise  $\mathcal{E}$ . For incoherent error such as the local depolarizing noise with uniform error rate  $\mathcal{E} = \bigcirc_{i=1}^n \mathcal{E}_{\text{dep}}^{(i)}$ , where  $\mathcal{E}_{\text{dep}}^{(i)}(\cdot) =$  $(1-\frac{3}{4}p)\cdot +\frac{p}{4}(X_i\cdot X_i+Y_i\cdot Y_i+Z_i\cdot Z_i)$  is the single-qubit local depolarizing channel on the *i*-th qubit, we obtain

$$\mathbb{E}_{U}[|R\operatorname{tr}[\mathcal{E}'(\rho)O] - \operatorname{tr}[\rho O]|] \le O(\sqrt{nL}p) \text{ with } R = (1 + O(p))^{nL}$$
(S37)

from Eq. (S34). Meanwhile, for coherent error  $\mathcal{E} = \bigcap_{i=1}^n \mathcal{E}_{\mathrm{coh}}^{(i)}$  with  $\|\mathcal{E}_{\mathrm{coh}}^{(i)} - \mathrm{Id}\|_{\diamond} = \epsilon_{\mathrm{coh}}$ , we obtain

$$\mathbb{E}_{U}[|R\mathrm{tr}[\mathcal{E}'(\rho)O] - \mathrm{tr}[\rho O]|] \le O(\sqrt{nL}\epsilon_{\mathrm{coh}}) \text{ with } R = (1 + O(\epsilon_{\mathrm{coh}}^{2}))^{nL}.$$
 (S38)

These results mean that, in terms of the sampling overhead  $R^2$ , coherent errors have quadratically suppressed sampling overhead compared to incoherent errors (see also Table S1). However, its effect on the bias is linear as in the case of incoherent errors. Therefore, it is preferable to suppress its error rate through randomized compiling or error crafting, and improve the performance of the white-noise approximation.

We can observe a similar scaling numerically. Before discussing the effect of the coherent noise, let us briefly summarize the numerical argument for incoherent noise, especially the local depolarizing noise  $\mathcal{E} = \bigcap_{i=1}^n \mathcal{E}_{\text{dep}}^{(i)}$ , provided in Ref. [33]. We analyze the convergence to white noise by examining the Pauli transfer matrix (PTM) of the effective noise  $\mathcal{E}'$ , denoted hereafter as  $\Gamma$ . We define  $\Gamma$  by  $\Gamma_{ij} = \text{Tr}[P_i\mathcal{E}'(P_j)]/2^n$  for  $P_i, P_j \in \{I, X, Y, Z\}^{\otimes n}$  for n-qubit system. Note that PTM is diagonal if  $\mathcal{E}'$  is a Pauli channel, and furthermore there exists  $0 \le w \le 1$  such that  $\Gamma_{ii} = w$   $(i \ne 0)$  if  $\mathcal{E}'$  is the white noise. In this regard, it is useful to compute the singular values of the PTM in order to investigate the closeness to the white noise. We in particular compute  $\Gamma = V\Lambda W^{\dagger}$  with  $\Lambda = \text{diag}\{\lambda_i\}_{i=1}^{4^n}$ , and define the damping factor  $k_i$  as follows,

$$\lambda_i = (1 - p)^{-k_i L}. \tag{S39}$$

It can be proven that, when each unitary layer consists of unitary 2-design, the damping factor converges to  $k_{\text{mean}} = \frac{3n}{4} \frac{4^n}{4^n-1}$ , and numerical analysis supports that this also holds for weaker randomness, e.g., 2-local random circuits with linear connectivity, when the circuit depth is sufficiently deep. In other words, the mean deviation  $\mathbb{E}_i[|k_i - k_{\text{mean}}|]$ , as well as the deviation of extremals  $|k_{\text{max}(\text{min})} - k_{\text{mean}}|$ , is suppressed as  $O(1/\sqrt{L})$  [33], which is consistent with the suppression of total variation distance in measurement probability distribution in the computational basis [54].

Now we ask how the above behavior is affected by the presence of coherent errors. Here, for the sake of simplicity of the argument, we sample  $U_i$  uniformly from the entire unitary group, i.e., take an n-qubit Haar random unitary, and consider a local noise as  $\mathcal{E}_l = \bigcap_{i=1}^n \mathcal{E}_{\text{coh}}^{(i)} \circ \mathcal{E}_{\text{dep}}^{(i)}$ , where  $\mathcal{E}_{\text{coh}}^{(i)}$  is a random 1-qubit unitary such that  $\|\mathcal{E}_{\text{coh}}^{(i)} - \text{Id}\|_{\diamond} = \epsilon_{\text{coh}}$ . In practice, this can be realized by constraining the rotation angles under the axial decomposition of the unitary.

Interestingly, we find that the effect of coherent error on the magnitude of the white noise is quadratically suppressed, while that on the convergence rate is linear. In Fig. S3(a)(b) we can see that, although the fluctuation in the damping factor is expanded at the shallow-depth regime, it readily converges at the rate of  $O(1/\sqrt{L})$ , which is in similar to the depolarizing-only case [33]. We observe that the deviation  $\max_k\{|k-k_{\text{mean,dep}}|\}$  is lifted approximately by a factor of  $(\epsilon_{\text{coh}} + \epsilon_{\text{dep}})/\epsilon_{\text{dep}}$  where  $\epsilon_{\text{dep}} := \|\mathcal{E}_{\text{dep}}^{(i)} - \text{Id}\|_{\diamond}$ , implying the slow down of the white noise convergence. Meanwhile, as shown in Fig. S3(c), we notice that the converged effective channel is less affected, in a sense that  $|k_{\text{mean,tot}} - k_{\text{mean,dep}}| \propto \epsilon^2$ . Phenomenologically, we can understand that the effect of coherent noise is self-twirled by the circuit such that the diamond norm is suppressed quadratically as in the random compilation scheme [43]. These results indicate that, although the presence of coherent error does not severely increase the sampling overhead to perform error countermeasures such as the rescaling technique, the adequacy of the approximation is degraded and hence desirable to avoid them by error-crafted synthesis.

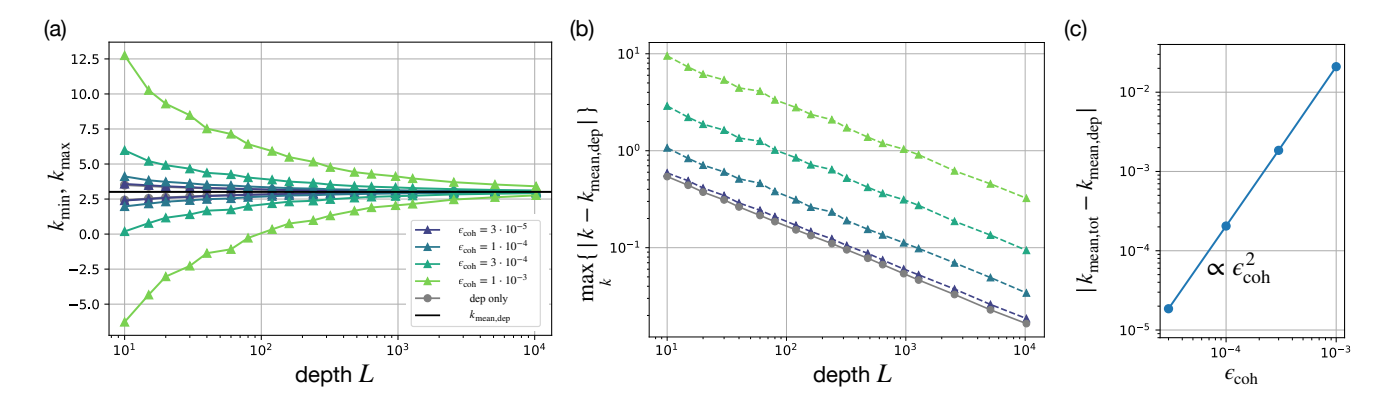


FIG. S3. Convergence to white noise in n=4 qubit quantum circuit. (a) Extremal values of damping factors  $k_{\min}$  and  $k_{\max}$  at various L. The unitary layer is drawn uniform-randomly from the n-qubit unitary group. Each layer is subject to error  $\bigcap_{i=1}^{N} \mathcal{E}_{\text{coh}} \circ \mathcal{E}_{\text{dep}}$  with depolarizing error rate of  $p=10^{-4}$ . (b) The largest deviation from  $k_{\text{mean,dep}}$ , the value realized when only the depolarizing noise is present ( $\epsilon_{\text{coh}}=0$ ). (c) The quadratic suppression of damping factor k with respect to the contribution from coherent noise. Here, we compute  $|k_{\text{mean,tot}}-k_{\text{mean,dep}}|$  at  $L=10^4$ .

#### S7. THEORETICAL GUARANTEES FOR ERROR CRAFTED SYNTHESIS

#### Crafting Pauli channel (Proof of Theorem 1)

In this section, we provide the formal statement and proof for Theorem 1 in the main text. First, we rewrite the Pauli-constrained minimization problem using the magic basis introduced in Sec. S2 to obtain the following,

minimize 
$$1 - \sum_{j} p_j \left(r_1^{(j)}\right)^2$$
 subject to  $\sum_{j} p_j = 1, p_j \ge 0, \sum_{j} p_j r^{(j)} r^{(j)T}$  is diagonal, (S40)

where  $r^{(j)}=(r_1^{(j)},r_2^{(j)},r_3^{(j)},r_4^{(j)})\in\mathbb{R}^4$  corresponds to the magic basis representation of the error channel for the j-th basis  $U_i \circ \hat{U}^{-1}$ . As we described in Sec. S2, this optimization can be solved by linear programming if the solution exists. Thus, the only nontrivial part for tailoring Pauli error is how to guarantee the existence of a solution. As we already mentioned in the main text, we rigorously guarantee the existence of such a basis set:

**Theorem S1.** (Detailed version of Theorem 1.) There exist a positive numbers  $c, \epsilon_0$  and unit vectors  $\{\vec{v}^{(j)} \in \mathbb{R}^3\}_{i=1}^7$ such that for any given single-qubit unitary  $\hat{\mathcal{U}}$  and for any  $\epsilon \in (0, \epsilon_0]$ , if we construct target unitaries  $\{\hat{\mathcal{U}}_j\}_{j=1}^7$  satisfying

$$\frac{1}{2} \left[ \mathcal{J}(\hat{\mathcal{U}}_j \circ \hat{\mathcal{U}}^{-1}) \right]_{MB} = \hat{e}^{(j)} \hat{e}^{(j)T} \quad \text{with} \quad \hat{e}^{(j)} = \begin{pmatrix} \sqrt{1 - (c\epsilon)^2} \\ c\epsilon \hat{\vec{v}}^{(j)} \end{pmatrix}$$
 (S41)

and obtain  $\{\mathcal{U}_j\}_j$  via unitary synthesis such that  $\frac{1}{2} \|\hat{\mathcal{U}}_j - \mathcal{U}_j\|_{\diamond} \leq \epsilon$ , then a solution in Eq. (S15) exists. Moreover, it holds that

$$((c-1)\epsilon)^2 \le \frac{1}{2} \left\| \hat{\mathcal{U}} - \sum_{j=1}^7 p_j \mathcal{U}_j \right\|_{\hat{\Omega}} \le ((c+1)\epsilon)^2$$
 (S42)

with the optimal probability distribution  $\{p_i\}$  that induces a Pauli synthesis error.

*Proof.* By letting  $r^{(j)}$  be the magic basis representation of  $\mathcal{U}_i \circ \hat{\mathcal{U}}^{-1}$  and defining

$$A_{L} = \begin{pmatrix} r_{1}^{(1)} r_{2}^{(1)} & r_{1}^{(2)} r_{2}^{(2)} & \cdots & r_{1}^{(L)} r_{2}^{(L)} \\ r_{1}^{(1)} r_{3}^{(1)} & r_{1}^{(2)} r_{3}^{(2)} & \cdots & r_{1}^{(L)} r_{3}^{(L)} \\ r_{1}^{(1)} r_{4}^{(1)} & r_{1}^{(2)} r_{3}^{(2)} & \cdots & r_{1}^{(L)} r_{4}^{(L)} \\ r_{1}^{(2)} r_{3}^{(1)} & r_{2}^{(2)} r_{3}^{(2)} & \cdots & r_{2}^{(L)} r_{3}^{(L)} \\ r_{2}^{(1)} r_{3}^{(1)} & r_{2}^{(2)} r_{3}^{(2)} & \cdots & r_{2}^{(L)} r_{4}^{(L)} \\ r_{3}^{(1)} r_{4}^{(1)} & r_{3}^{(2)} r_{4}^{(2)} & \cdots & r_{3}^{(L)} r_{4}^{(L)} \end{pmatrix} = \begin{pmatrix} m^{(1)} & m^{(2)} & \cdots & m^{(L)} \end{pmatrix},$$
(S43)

we can describe the non-diagonal elements in  $\sum_{j=1}^{L} p_j r^{(j)} r^{(j)T}$  obtained by mixing  $\{\mathcal{U}_j\}_{j=1}^{L}$  as a vector  $A_L p$ . Suppose that  $A_6$  is invertible. Then, it is sufficient to show  $(A_6^{-1} m^{(7)})_i \leq 0$  for any  $i \in \{1, \dots, 6\}$ . This is because  $\mathbf{e}^{(i)T}A_6^{-1}m^{(k)} = \delta_{ik}$ , where  $\delta_{ik}$  is the Kronecker delta and  $\mathbf{e}^{(i)}$  is the unit vector whose element is 0 except the *i*-th element.

$$\forall i \in \{1, \dots, 6\}, \mathbf{e}^{(i)T} A_6^{-1} m^{(7)} \le 0 \iff \exists \tilde{p} : \{1, \dots, 6\} \to [0, \infty), m^{(7)} = -\sum_{i=1}^{6} \tilde{p}_j m^{(j)}, \tag{S44}$$

and we can verify  $A_7p=0$  by setting  $p_j=\frac{\tilde{p}_j}{1+\sum_{i'=1}^6\tilde{p}_{j'}}$  for  $j\in\{1,\cdots,6\}$  and  $p_7=\frac{1}{1+\sum_{j=1}^6\tilde{p}_j}$ .

In the following, we show that  $A_6$  is invertible and  $\max_i (A_6^{-1} m^{(7)})_i \leq 0$  by using the continuity of the matrix inverse. Define  $D = diag(\frac{1}{c\epsilon\sqrt{1-(c\epsilon)^2}}, \frac{1}{c\epsilon\sqrt{1-(c\epsilon)^2}}, \frac{1}{c\epsilon\sqrt{1-(c\epsilon)^2}}, \frac{1}{(c\epsilon)^2}, \frac{1}{(c\epsilon)^2}, \frac{1}{(c\epsilon)^2}, \frac{1}{(c\epsilon)^2})$ . By letting

$$\hat{\vec{v}}^{(1)} = \begin{pmatrix} -1 \\ 0 \\ 0 \end{pmatrix}, \hat{\vec{v}}^{(2)} = \begin{pmatrix} 0 \\ -1 \\ 0 \end{pmatrix}, \hat{\vec{v}}^{(3)} = \begin{pmatrix} 0 \\ 0 \\ 1 \end{pmatrix}, \hat{\vec{v}}^{(4)} = \frac{1}{\sqrt{2}} \begin{pmatrix} 1 \\ -1 \\ 0 \end{pmatrix}, \hat{\vec{v}}^{(5)} = \frac{1}{\sqrt{2}} \begin{pmatrix} -1 \\ 0 \\ -1 \end{pmatrix}, \hat{\vec{v}}^{(6)} = \frac{1}{\sqrt{2}} \begin{pmatrix} 0 \\ 1 \\ 1 \end{pmatrix}, \hat{\vec{v}}^{(7)} = \frac{1}{\sqrt{3}} \begin{pmatrix} 1 \\ 1 \\ -1 \end{pmatrix},$$
(S45)

we can verify that

$$D\hat{A}_{6} = \begin{pmatrix} -1 & 0 & 0 & \frac{1}{\sqrt{2}} & -\frac{1}{\sqrt{2}} & 0 \\ 0 & -1 & 0 & -\frac{1}{\sqrt{2}} & 0 & \frac{1}{\sqrt{2}} \\ 0 & 0 & 1 & 0 & -\frac{1}{\sqrt{2}} & \frac{1}{\sqrt{2}} \\ 0 & 0 & 0 & -\frac{1}{2} & 0 & 0 \\ 0 & 0 & 0 & 0 & \frac{1}{2} & 0 \\ 0 & 0 & 0 & 0 & 0 & \frac{1}{2} \end{pmatrix}, (D\hat{A}_{6})^{-1} = \begin{pmatrix} -1 & 0 & 0 & -\sqrt{2} & -\sqrt{2} & 0 \\ 0 & -1 & 0 & \sqrt{2} & 0 & \sqrt{2} \\ 0 & 0 & 1 & 0 & \sqrt{2} & -\sqrt{2} \\ 0 & 0 & 0 & -2 & 0 & 0 \\ 0 & 0 & 0 & 0 & 2 & 0 \\ 0 & 0 & 0 & 0 & 2 & 0 \\ 0 & 0 & 0 & 0 & 0 & 2 \end{pmatrix}, \hat{A}_{6}^{-1}\hat{m}^{(7)} = -\frac{1}{3} \begin{pmatrix} \sqrt{3} \\ \sqrt{3} \\ \sqrt{3} \\ 2 \\ 2 \\ 2 \end{pmatrix}, (S46)$$

where  $\hat{A}_6$  is the matrix defined in the same way as Eq. (S43) for  $\hat{\mathcal{U}}_j \circ \hat{\mathcal{U}}^{-1}$ , and we use  $\hat{A}_6^{-1}\hat{m}^{(7)} = (D\hat{A}_6)^{-1}D\hat{m}^{(7)}$  in the last equality. Note that  $\hat{A}_6$  also allows us to determine  $\hat{m}^{(i)}$  (i=1,...,6). If we can show that there exists an upper bound  $u(c,\epsilon)$  of  $\|Dm^{(j)} - D\hat{m}^{(j)}\|_2$  satisfying

$$\forall j, \left\| Dm^{(j)} - D\hat{m}^{(j)} \right\|_{2} \le u(c, \epsilon) \quad \wedge \quad \lim_{c \to \infty} \lim_{\epsilon \to 0} u(c, \epsilon) = 0, \tag{S47}$$

it implies that  $DA_6$  is invertible ( $\Leftrightarrow A_6$  is invertible) and  $\max_i (A_6^{-1} m^{(7)})_i = \max_i ((DA_6)^{-1} D m^{(7)})_i \leq 0$  for large enough c and small enough  $\epsilon$  since  $D\hat{A}_6$  is a constant invertible matrix (independent to  $\epsilon$ ),  $\max_i ((D\hat{A}_6)^{-1} D \hat{m}^{(7)})_i = -\frac{1}{\sqrt{3}}$ , the set of invertible matrices is open, and  $f: A \to A^{-1}$  is continuous.

In the following, we assume that c > 1 and  $\epsilon_0 < \frac{1}{2c}$  and consider the case when  $\epsilon \in (0, \epsilon_0]$ . Let  $\sin \hat{\theta} = c\epsilon$ ,  $\sin \theta_0 = \epsilon$  and  $r^{(j)} = (\cos \theta_j, \sin \theta_j \vec{v}^{(j)})^T$  with  $\hat{\theta}, \theta_0 \in (0, \pi/6), \theta_j \in [0, \pi/2]$ . Since the following argument holds for any j, we abbreviate a subscript or superscript indicating a label j. From the assumption of compilation accuracy, we obtain

$$\cos \theta_0 = \sqrt{1 - \epsilon^2} \le |e \cdot \hat{e}| = |\cos \theta \cos \hat{\theta} + \sin \theta \sin \hat{\theta} \vec{v} \cdot \hat{\vec{v}}| = \cos \theta \cos \hat{\theta} + \sin \theta \sin \hat{\theta} \vec{v} \cdot \hat{\vec{v}}, \tag{S48}$$

where we use  $\theta < \frac{\pi}{3}$  (due to  $|\theta - \hat{\theta}| < \theta_0$ ) in the last equality. By using  $\theta > 0$  (due to c > 1), this is equivalent to

$$|\theta - \hat{\theta}| \le \theta_0 \land \vec{v} \cdot \hat{\vec{v}} \ge \frac{\cos \theta_0 - \cos \theta \cos \hat{\theta}}{\sin \theta \sin \hat{\theta}} (> 0). \tag{S49}$$

On the other hand,

$$||D(m - \hat{m})||_{2} = \sqrt{\left\|\hat{\vec{v}} - \frac{\cos\theta\sin\theta}{\cos\hat{\theta}\sin\hat{\theta}}\vec{v}\right\|_{2}^{2} + \left\|\left(\frac{\hat{v}_{1}\hat{v}_{2}}{\hat{v}_{1}\hat{v}_{3}}\right) - \left(\frac{\sin\theta}{\sin\hat{\theta}}\right)^{2} \begin{pmatrix}v_{1}v_{2}\\v_{1}v_{3}\\v_{2}v_{3}\end{pmatrix}\right\|_{2}^{2}}$$

$$= \sqrt{\left\|\hat{\vec{v}} - \frac{\sin(2\theta)}{\sin(2\hat{\theta})}\vec{v}\right\|_{2}^{2} + \frac{1}{2}\left(\left\|\hat{\vec{v}}\hat{\vec{v}}^{T} - \left(\frac{\sin\theta}{\sin\hat{\theta}}\right)^{2}\vec{v}\vec{v}^{T}\right\|_{2}^{2} - \sum_{i=1}^{3}\left(\hat{v}_{i}^{2} - \left(\frac{\sin\theta}{\sin\hat{\theta}}\right)^{2}v_{i}^{2}\right)^{2}}$$

$$\leq \sqrt{\left\|\hat{\vec{v}} - \frac{\sin(2\theta)}{\sin(2\hat{\theta})}\vec{v}\right\|_{2}^{2} + \frac{1}{2}\left(\left\|\hat{\vec{v}}\hat{\vec{v}}^{T} - \left(\frac{\sin\theta}{\sin\hat{\theta}}\right)^{2}\vec{v}\vec{v}^{T}\right\|_{2}^{2} - \frac{1}{3}\left(1 - \left(\frac{\sin\theta}{\sin\hat{\theta}}\right)^{2}\right)^{2}},$$
(S52)

where we use the Cauchy-Schwartz inequality  $\left(\sum_{i=1}^{3} \left(\hat{v}_{i}^{2} - \frac{\sin^{2}\theta}{\sin^{2}\hat{\theta}}v_{i}^{2}\right)^{2}\right) \left(\sum_{i=1}^{3} \left(\frac{1}{\sqrt{3}}\right)^{2}\right) = \sum_{i=1}^{3} \frac{1}{\sqrt{3}} \left(\hat{v}_{i}^{2} - \frac{\sin^{2}\theta}{\sin^{2}\hat{\theta}}v_{i}^{2}\right)^{2}$  in the last inequality. We proceed with the calculation as follows:

$$Eq. (S52) = \sqrt{1 + \left(\frac{\sin(2\theta)}{\sin(2\hat{\theta})}\right)^2 - 2\frac{\sin(2\theta)}{\sin(2\hat{\theta})}\vec{v} \cdot \hat{\vec{v}} + \frac{1}{2}\left(1 + \left(\frac{\sin\theta}{\sin\hat{\theta}}\right)^4 - 2\left(\frac{\sin\theta}{\sin\hat{\theta}}\vec{v} \cdot \hat{\vec{v}}\right)^2\right) - \frac{1}{6}\left(1 - \left(\frac{\sin\theta}{\sin\hat{\theta}}\right)^2\right)^2}.$$
(S53)

By using Eq. (S49), we obtain

$$\|D(m-\hat{m})\|_2 \le \max_{|\theta-\hat{\theta}| \le \theta_0} \sqrt{f(\hat{\theta},\theta,\theta_0)} = \sqrt{\max_{|t| \le 1} f(\hat{\theta},\theta_0t+\hat{\theta},\theta_0)}, \tag{S54}$$

where 
$$f(\hat{\theta}, \theta, \theta_0) = 1 + \left(\frac{\sin(2\theta)}{\sin(2\hat{\theta})}\right)^2 - 2\frac{\sin(2\theta)}{\sin(2\hat{\theta})}\frac{\cos\theta_0 - \cos\theta\cos\hat{\theta}}{\sin\theta\sin\hat{\theta}} + \frac{1}{2}\left(1 + \left(\frac{\sin\theta}{\sin\hat{\theta}}\right)^4 - 2\left(\frac{\cos\theta_0 - \cos\theta\cos\hat{\theta}}{\sin^2\hat{\theta}}\right)^2\right) - \frac{1}{6}\left(1 - \left(\frac{\sin\theta}{\sin\hat{\theta}}\right)^2\right)^2$$
. Define  $g_c(\epsilon, t) := f(\sin^{-1}(c\epsilon), \sin^{-1}(\epsilon)t + \sin^{-1}(c\epsilon), \sin^{-1}(\epsilon)t)$  on  $(\epsilon, t) \in (0, \epsilon_0] \times [-1, 1]$ . To complete the proof of Eq. (S47), it is sufficient to show  $\lim_{\epsilon \to 0} \max_{|t| \le 1} g_c(\epsilon, t) = 0$ . As shown in Section S8 A,  $g_c(\epsilon, t)$  is uniformly continuous in  $(\epsilon, t) \in (0, \epsilon_0] \times [-1, 1]$ . Thus, we can interchange  $\lim_{\epsilon \to 0}$  and  $\max_{|t| \le 1}$  (see detail in Section S8 B) and obtain

$$\lim_{\epsilon \to 0} \max_{|t| < 1} g_c(\epsilon, t) = \max_{|t| < 1} \lim_{\epsilon \to 0} g_c(\epsilon, t)$$
(S55)

$$= \max_{|t| \le 1} \frac{1}{c^4} \left( \frac{1}{12} t^4 + \frac{c}{3} t^3 + \left( \frac{c^2}{3} + \frac{1}{2} \right) t^2 + ct + 2c^2 - \frac{1}{4} \right)$$
 (S56)

$$= \frac{7}{3c^2} + \frac{4}{3c^3} + \frac{1}{3c^4},\tag{S57}$$

where the last equality is obtained by observing that t = 1 maximizes the polynomial via a straightforward calculation. Finally, we obtain

$$||Dm - D\hat{m}||_2 \le u(c, \epsilon) \wedge \lim_{\epsilon \to 0} u(c, \epsilon) = \sqrt{\frac{7}{3c^2} + \frac{4}{3c^3} + \frac{1}{3c^4}}.$$
 (S58)

This completes the proof.

# B. Crafting depolarizing channel

In similar to the Pauli constraint, the minimization problem to obtain the synthesis probability distribution under the depolarizing constraint can be written as

minimize 
$$\frac{1}{2} \left\| \hat{\mathcal{U}} - \sum_{j} p_{j} \mathcal{U}_{j} \right\|_{\circ}$$
 subject to  $\sum_{a} \chi_{aa} = 1, \chi_{XX} = \chi_{YY} = \chi_{ZZ} = q \ge 0, \chi_{a \ne b} = 0,$  (S59)

which is rewritten under the magic basis representation as

minimize 
$$1 - \sum_{j} p_j \left(r_1^{(j)}\right)^2$$
 subject to  $\sum_{j} p_j = 1, p_j \ge 0, \sum_{j} p_j r^{(j)} r^{(j)T} = (1 - q) \mathbf{e}^{(1)} \mathbf{e}^{(1)T} + \frac{q}{4} \mathrm{Id},$  (S60)

where  $r^{(j)} \in \mathbb{R}^4$  corresponds to the magic basis representation of  $\mathcal{U}_j \circ \hat{\mathcal{U}}^{-1}$  given in Eq. (S12), and  $\mathbf{e}^{(i)}$  is the unit vector whose element is 0 except the *i*-th element.

We can prove the feasibility guarantee as in the following theorem:

**Theorem S2.** There exist positive numbers c,  $\epsilon_0$  and unit vectors  $\{\hat{v}^{(j)} \in \mathbb{R}^3\}_{j=1}^9$  such that for any given single-qubit unitary  $\hat{\mathcal{U}}$  and for any  $\epsilon \in (0, \epsilon_0]$ , if we prepare target unitaries  $\{\hat{\mathcal{U}}_j\}_{j=1}^9$  satisfying

$$\frac{1}{2} \left[ \mathcal{J}(\hat{\mathcal{U}}_j \circ \hat{\mathcal{U}}^{-1}) \right]_{MB} = \hat{e}^{(j)} \hat{e}^{(j)T} \quad \text{with} \quad \hat{e}^{(j)} = \begin{pmatrix} \sqrt{1 - (c\epsilon)^2} \\ c\epsilon \hat{\vec{v}}^{(j)} \end{pmatrix}$$
 (S61)

and obtain  $\{\mathcal{U}_j\}_j$  via unitary synthesis such that  $\frac{1}{2} \|\hat{\mathcal{U}}_j - \mathcal{U}_j\|_{\diamond} \leq \epsilon$ , then a solution in Eq. (S59) exists. Moreover, it holds that

$$((c-1)\epsilon)^2 \le \frac{1}{2} \left\| \hat{\mathcal{U}} - \sum_{j=1}^9 p_j \mathcal{U}_j \right\|_{\circ} \le ((c+1)\epsilon)^2$$
 (S62)

with the optimal probability distribution  $\{p_i\}$  that induces a depolarizing channel as the effective synthesis error.

*Proof.* By letting  $r^{(j)}$  be the magic basis representation of  $\mathcal{U}_j \circ \hat{\mathcal{U}}^{-1}$  and defining

$$A_{L} = \begin{pmatrix} r_{1}^{(1)}r_{2}^{(1)} & r_{1}^{(2)}r_{2}^{(2)} & \cdots & r_{1}^{(L)}r_{2}^{(L)} \\ r_{1}^{(1)}r_{3}^{(1)} & r_{1}^{(2)}r_{3}^{(2)} & \cdots & r_{1}^{(L)}r_{3}^{(L)} \\ r_{1}^{(1)}r_{3}^{(1)} & r_{1}^{(2)}r_{3}^{(2)} & \cdots & r_{1}^{(L)}r_{3}^{(L)} \\ r_{1}^{(1)}r_{4}^{(1)} & r_{1}^{(2)}r_{4}^{(2)} & \cdots & r_{1}^{(L)}r_{4}^{(L)} \\ r_{2}^{(1)}r_{3}^{(1)} & r_{2}^{(2)}r_{3}^{(2)} & \cdots & r_{2}^{(L)}r_{3}^{(L)} \\ r_{2}^{(1)}r_{4}^{(1)} & r_{2}^{(2)}r_{4}^{(2)} & \cdots & r_{2}^{(L)}r_{4}^{(L)} \\ r_{3}^{(1)}r_{4}^{(1)} & r_{3}^{(2)}r_{4}^{(2)} & \cdots & r_{3}^{(L)}r_{4}^{(L)} \\ (r_{2}^{(1)})^{2} - (r_{3}^{(1)})^{2} & (r_{2}^{(2)})^{2} - (r_{3}^{(2)})^{2} & \cdots & (r_{2}^{(L)})^{2} - (r_{3}^{(L)})^{2} \\ (r_{2}^{(1)})^{2} - (r_{4}^{(1)})^{2} & (r_{2}^{(2)})^{2} - (r_{4}^{(2)})^{2} & \cdots & (r_{2}^{(L)})^{2} - (r_{4}^{(L)})^{2} \end{pmatrix}$$

$$(S63)$$

we can describe the restrictions about the depolarizing error obtained by mixing  $\{\mathcal{U}_j\}_{j=1}^L$  as  $A_L p = 0$ . Define  $D = diag(\frac{1}{c\epsilon\sqrt{1-(c\epsilon)^2}}, \frac{1}{c\epsilon\sqrt{1-(c\epsilon)^2}}, \frac{1}{c\epsilon\sqrt{1-(c\epsilon)^2}}, \frac{1}{(c\epsilon)^2}, \frac{1}{(c\epsilon)^2}, \frac{1}{(c\epsilon)^2}, \frac{1}{\sqrt{8}(c\epsilon)^2}, \frac{1}{\sqrt{8}(c\epsilon)^2})$ . Suppose that  $DA_8$  is invertible. Then, it is sufficient to show  $((DA_8)^{-1}(Dm^{(9)}))_i \leq 0$  for any  $i \in \{1, \cdots, 8\}$  and  $\{r^{(j)}\}_{j=1}^9$ . We can find  $\{\hat{v}^{(x)}\}_{x=1}^9$ satisfying the conditions such that  $D\hat{A}_8$  is a constant invertible matrix and  $\max_i((D\hat{A}_8)^{-1}(D\hat{m}^{(9)}))_i$  is a constant negative real. For example, by setting

$$\hat{\vec{v}}^{(1)} = \begin{pmatrix} 1\\0\\0 \end{pmatrix}, \hat{\vec{v}}^{(2)} = \begin{pmatrix} -1\\0\\0 \end{pmatrix}, \hat{\vec{v}}^{(3)} = \begin{pmatrix} 0\\-1\\0 \end{pmatrix}, \hat{\vec{v}}^{(4)} = \begin{pmatrix} 0\\0\\1 \end{pmatrix}, \hat{\vec{v}}^{(5)} = \begin{pmatrix} 0\\0\\-1 \end{pmatrix}, 
\hat{\vec{v}}^{(6)} = \frac{1}{\sqrt{2}} \begin{pmatrix} -1\\0\\-1 \end{pmatrix}, \hat{\vec{v}}^{(7)} = \frac{1}{\sqrt{2}} \begin{pmatrix} 0\\1\\1 \end{pmatrix}, \hat{\vec{v}}^{(8)} = \frac{1}{\sqrt{2}} \begin{pmatrix} -1\\1\\0 \end{pmatrix}, \hat{\vec{v}}^{(7)} = \frac{1}{\sqrt{3}} \begin{pmatrix} 1\\1\\-1 \end{pmatrix},$$
(S64)

we can verify the conditions are satisfied. This is because

$$D\hat{A}_8 = \begin{pmatrix} 1 & -1 & 0 & 0 & 0 & -\frac{1}{\sqrt{2}} & 0 & -\frac{1}{\sqrt{2}} \\ 0 & 0 & -1 & 0 & 0 & 0 & \frac{1}{\sqrt{2}} & \frac{1}{\sqrt{2}} \\ 0 & 0 & 0 & 1 & -1 & -\frac{1}{\sqrt{2}} & \frac{1}{\sqrt{2}} & 0 \\ 0 & 0 & 0 & 0 & 0 & 0 & 0 & -\frac{1}{2} \\ 0 & 0 & 0 & 0 & 0 & \frac{1}{2} & 0 & 0 \\ 0 & 0 & 0 & 0 & 0 & 0 & \frac{1}{2} & 0 \\ 0 & 0 & 0 & 0 & 0 & 0 & \frac{1}{2} & 0 \\ \frac{1}{2\sqrt{2}} & \frac{1}{2\sqrt{2}} & -\frac{1}{2\sqrt{2}} & 0 & 0 & \frac{1}{4\sqrt{2}} & -\frac{1}{4\sqrt{2}} & 0 \\ \frac{1}{2\sqrt{2}} & \frac{1}{2\sqrt{2}} & 0 & -\frac{1}{2\sqrt{2}} & -\frac{1}{2\sqrt{2}} & 0 & -\frac{1}{4\sqrt{2}} & \frac{1}{4\sqrt{2}} \end{pmatrix},$$

$$(D\hat{A}_{8})^{-1} = \begin{pmatrix} \frac{1}{2} & -\frac{1}{2} & 0 & -\sqrt{2} & -\frac{1}{2} + \frac{1}{\sqrt{2}} & \frac{1}{2} + \frac{1}{\sqrt{2}} & \sqrt{2} & 0 \\ -\frac{1}{2} & -\frac{1}{2} & 0 & 0 & -\frac{1}{2} - \frac{1}{2} + \frac{1}{\sqrt{2}} & \sqrt{2} & 0 \\ 0 & -1 & 0 & -\sqrt{2} & 0 & \sqrt{2} & 0 & 0 \\ 0 & -\frac{1}{2} & \frac{1}{2} & -\frac{1}{2} - \frac{1}{2} - \frac{1}{2} + \frac{1}{\sqrt{2}} & 0 & \sqrt{2} - \sqrt{2} \\ 0 & -\frac{1}{2} & -\frac{1}{2} & -\frac{1}{2} - \frac{1}{2} - \frac{1}{2} - \frac{1}{\sqrt{2}} & -\frac{1}{2} - \frac{1}{\sqrt{2}} & \sqrt{2} & \sqrt{2} \\ 0 & 0 & 0 & 0 & 2 & 0 & 0 & 0 \\ 0 & 0 & 0 & 0 & 2 & 0 & 0 & 0 \\ 0 & 0 & 0 & 0 & -2 & 0 & 0 & 0 & 0 \end{pmatrix}, \hat{A}_{8}^{-1}\hat{m}^{(9)} = -\frac{1}{3} \begin{pmatrix} 2\sqrt{2} \\ \sqrt{3} \\ 2\sqrt{2} \\ \sqrt{3} \\ \sqrt{2} + \sqrt{3} \\ \sqrt{2} \\ 2 \\ 2 \\ 2 \end{pmatrix}, \tag{S65}$$

where we use  $\hat{A}_8^{-1}\hat{m}^{(9)}=(D\hat{A}_8)^{-1}D\hat{m}^{(9)}$  in the last equality.

Thus, it is sufficient to show there exists an upper bound  $u(c,\epsilon)$  of  $\|Dm^{(j)} - D\hat{m}^{(j)}\|_2$  satisfying

$$\left\|Dm^{(j)} - D\hat{m}^{(j)}\right\|_{2} \le u(c,\epsilon) \quad \wedge \quad \lim_{c \to \infty} \lim_{\epsilon \to 0} u(c,\epsilon) = 0, \tag{S66}$$

In the following, we assume that c > 1 and  $\epsilon_0 < \frac{1}{2c}$  and consider the case when  $\epsilon \in (0, \epsilon_0]$ . Let  $\sin \hat{\theta} = c\epsilon$ ,  $\sin \theta_0 = \epsilon$  and  $r^{(j)} = (\cos \theta_j, \sin \theta_j \vec{v}^{(j)})^T$  with  $\hat{\theta}, \theta_0 \in (0, \pi/6), \theta_x \in [0, \pi/2]$ . Since the following argument holds for any j, we abbreviate a subscript or superscript indicating a label j. From the assumption of compilation accuracy, we obtain

$$|\theta - \hat{\theta}| \le \theta_0 \land \vec{v} \cdot \hat{\vec{v}} \ge \frac{\cos \theta_0 - \cos \theta \cos \hat{\theta}}{\sin \theta \sin \hat{\theta}} (> 0). \tag{S67}$$

On the other hand,

$$\begin{split} \|D(m-\hat{m})\|_{2}^{2} &= \left\|\hat{\vec{v}} - \frac{\cos\theta\sin\theta}{\cos\hat{\theta}\sin\hat{\theta}}\vec{\vec{v}}\right\|_{2}^{2} + \left\|\begin{pmatrix}\hat{v}_{1}\hat{v}_{2}\\\hat{v}_{1}\hat{v}_{3}\\\hat{v}_{2}\hat{v}_{3}\end{pmatrix} - \left(\frac{\sin\theta}{\sin\hat{\theta}}\right)^{2}\begin{pmatrix}v_{1}v_{2}\\v_{1}v_{3}\\v_{2}v_{3}\end{pmatrix}\right\|_{2}^{2} + \frac{1}{8}\left\|\begin{pmatrix}\hat{v}_{1}^{2} - \hat{v}_{2}^{2}\\\hat{v}_{1}^{2} - \hat{v}_{3}^{2}\end{pmatrix} - \left(\frac{\sin\theta}{\sin\hat{\theta}}\right)^{2}\begin{pmatrix}v_{1}^{2} - v_{2}^{2}\\v_{1}^{2} - v_{3}^{2}\end{pmatrix}\right\|_{2}^{2} \\ & (S68) \end{split}$$

$$&= \left\|\hat{\vec{v}} - \frac{\sin(2\theta)}{\sin(2\hat{\theta})}\vec{\vec{v}}\right\|_{2}^{2} + \frac{1}{2}\left(\left\|\hat{\vec{v}}\hat{\vec{v}}^{T} - \left(\frac{\sin\theta}{\sin\hat{\theta}}\right)^{2}\vec{v}\vec{v}^{T}\right\|_{2}^{2} - \sum_{i=1}^{3}r_{i}^{2}\right) + \frac{1}{8}\left((r_{1} - r_{2})^{2} + (r_{1} - r_{3})^{2}\right) \\ &\leq \left\|\hat{\vec{v}} - \frac{\sin(2\theta)}{\sin(2\hat{\theta})}\vec{\vec{v}}\right\|_{2}^{2} + \frac{1}{2}\left\|\hat{\vec{v}}\hat{\vec{v}}^{T} - \left(\frac{\sin\theta}{\sin\hat{\theta}}\right)^{2}\vec{v}\vec{v}^{T}\right\|_{2}^{2} + \frac{(r_{1} - r_{2})^{2} + (r_{1} - r_{3})^{2} + (r_{2} - r_{3})^{2} - 4\sum_{i=1}^{3}r_{i}^{2}}{8} \\ &= \left\|\hat{\vec{v}} - \frac{\sin(2\theta)}{\sin(2\hat{\theta})}\vec{v}\right\|_{2}^{2} + \frac{1}{2}\left\|\hat{\vec{v}}\hat{\vec{v}}^{T} - \left(\frac{\sin\theta}{\sin\hat{\theta}}\right)^{2}\vec{v}\vec{v}^{T}\right\|_{2}^{2} - \frac{(r_{1} + r_{2})^{2} + (r_{1} + r_{3})^{2} + (r_{2} + r_{3})^{2}}{8} \\ &\leq \left\|\hat{\vec{v}} - \frac{\sin(2\theta)}{\sin(2\hat{\theta})}\vec{v}\right\|_{2}^{2} + \frac{1}{2}\left\|\hat{\vec{v}}\hat{\vec{v}}^{T} - \left(\frac{\sin\theta}{\sin\hat{\theta}}\right)^{2}\vec{v}\vec{v}^{T}\right\|_{2}^{2} - \frac{1}{6}\left(1 - \left(\frac{\sin\theta}{\sin\hat{\theta}}\right)^{2}\right)^{2}, \end{aligned} \tag{S71}$$

where we let  $r_i = \hat{v}_i^2 - \left(\frac{\sin\theta}{\sin\hat{\theta}}\right)^2 v_i^2$  and we use the Cauchy-Schwartz inequality

$$\left( (r_1 + r_2)^2 + (r_1 + r_3)^2 + (r_2 + r_3)^2 \right) \left( \sum_{i=1}^3 \left( \frac{1}{\sqrt{3}} \right)^2 \right) \ge \left( \frac{r_1 + r_2}{\sqrt{3}} + \frac{r_1 + r_3}{\sqrt{3}} + \frac{r_2 + r_3}{\sqrt{3}} \right)^2 = \frac{4}{3} \left( 1 - \left( \frac{\sin \theta}{\sin \hat{\theta}} \right)^2 \right)^2 (S73)$$

By using the same argument as in Sec. S7A, we obtain

$$||Dm - D\hat{m}||_2 \le u(c, \epsilon) \wedge \lim_{\epsilon \to 0} u(c, \epsilon) = \sqrt{\frac{7}{3c^2} + \frac{4}{3c^3} + \frac{1}{3c^4}}.$$
 (S74)

This completes the proof of Eq. (S66).

#### S8. TECHNICAL LEMMAS

# A. Uniform continuity of $g_c(\epsilon, t)$

Since the summation f+g, the product fg and the composition  $f\circ g$  of two bounded uniformly continuous functions f and g are bounded and uniformly continuous, we can show the uniform continuity of  $g_c(\epsilon,t)$  by observing that its each term is bounded and uniformly continuous on  $(\epsilon,t)\in(0,\epsilon_0]\times[-1,1]$  with  $\epsilon_0<\frac{1}{2c}$  and c>1 as follows:

- 1.  $\theta = \sin^{-1}(\epsilon)t + \sin^{-1}(c\epsilon)$ ,  $\hat{\theta} = \sin^{-1}(c\epsilon)$  and  $\theta_0 = \sin^{-1}(\epsilon)$  are bounded and uniformly continuous, whose range lies in  $(0, \frac{\pi}{3})$ .
- 2.  $\frac{\theta_0}{\hat{\theta}} = \frac{1}{c} \frac{\sin^{-1}(\epsilon)}{\epsilon} \frac{c\epsilon}{\sin^{-1}(c\epsilon)}$  and  $\frac{\theta}{\hat{\theta}} = \frac{\theta_0}{\hat{\theta}}t + 1$  are bounded and uniformly continuous since  $\frac{\sin^{-1}(r)}{r}$  and  $\frac{r}{\sin^{-1}(r)}$  are bounded and uniformly continuous on  $r \in (0,1]$ . Since both ranges of  $\frac{\theta_0}{\hat{\theta}}$  and  $\frac{\theta}{\hat{\theta}}$  are included in a closed interval

 $[a,b]\subset (0,\infty)$  and  $f(r)=\frac{1}{r}$  is bounded and uniformly continuous on  $r\in [a,b]$ ,  $\frac{\hat{\theta}}{\theta_0}$  and  $\frac{\hat{\theta}}{\theta}$  are also bounded and uniformly continuous. By using the similar argument, we can verify that  $\frac{\theta}{\theta_0}=t+\frac{\hat{\theta}}{\theta_0}$  and  $\frac{\theta_0}{\theta}$  are bounded and uniformly continuous.

- 3.  $\frac{\sin \theta}{\sin \hat{\theta}} = \frac{\sin \theta}{\theta} \frac{\hat{\theta}}{\sin \hat{\theta}} \frac{\theta}{\hat{\theta}}$  and  $\frac{\sin(2\theta)}{\sin(2\hat{\theta})} = \frac{\sin(2\theta)}{2\theta} \frac{2\hat{\theta}}{\sin(2\hat{\theta})} \frac{\theta}{\hat{\theta}}$  are bounded and uniformly continuous since  $\frac{\sin \phi}{\phi}$  and  $\frac{\phi}{\sin \phi}$  are bounded and uniformly continuous on  $\phi \in (0, \frac{2\pi}{3})$ .
- 4.  $\frac{\cos\theta_0 \cos\theta\cos\hat{\theta}}{\sin\theta\sin\hat{\theta}} = \frac{\theta}{\sin\theta}\frac{\hat{\theta}}{\sin\hat{\theta}}\left(\frac{\theta_0}{\theta}\frac{\theta_0}{\hat{\theta}}\frac{\cos\theta_0 1}{\theta^2} \frac{\hat{\theta}}{\theta}\frac{\cos\hat{\theta} 1}{\hat{\theta}^2} + \frac{\theta}{\hat{\theta}}\frac{(1 \cos\theta)}{\theta^2}\cos\hat{\theta}\right) \text{ is bounded and uniformly continuous since } \frac{\cos\phi 1}{\phi^2} \text{ is bounded and uniformly continuous on } \phi \in (0, \frac{\pi}{3}).$

#### B. Commutativity of lim and max for uniformly continuous functions

Let E and T be an arbitrary subset and a compact subset of  $\mathbb{R}$ , respectively. Let  $\epsilon_0$  be a limit point of E and  $g: E \times T \to \mathbb{R}$  be uniformly continuous such that  $\lim_{\epsilon \to \epsilon_0} g(\epsilon, t)$  is finite for all  $t \in T$ . Then, we can show that

$$\lim_{\epsilon \to \epsilon_0} \max_{t \in T} g(\epsilon, t) = \max_{t \in T} \lim_{\epsilon \to \epsilon_0} g(\epsilon, t). \tag{S75}$$

Note that the 'uniform' continuity is requisite, e.g.,  $\lim_{\epsilon \to 0} \max_{t \in T} g(\epsilon, t) = 1$  and  $\max_{t \in T} \lim_{\epsilon \to 0} g(\epsilon, t) = 0$  for T = [0, 1], E = (0, 1), and g is a continuous function such that supp (g) is included in  $\{(\epsilon, t) : t < \epsilon < 4t\}$  and  $g(\epsilon, t) = 1$  if  $2t \le \epsilon \le 3t$ .

*Proof.* First, we can verify that  $f(t) := \lim_{\epsilon \to \epsilon_0} g(\epsilon, t)$  and  $h(\epsilon) := \max_{t \in T} g(\epsilon, t)$  are uniformly continuous as follows. Since g is uniformly continuous, for any  $\Delta > 0$ , there exists  $\delta > 0$  such that for any  $t, t' \in T$  and  $\epsilon, \epsilon' > 0$ , if

$$\left\| \begin{pmatrix} \epsilon \\ t \end{pmatrix} - \begin{pmatrix} \epsilon' \\ t' \end{pmatrix} \right\|_2 < \delta, |g(\epsilon, t) - g(\epsilon', t')| < \Delta. \text{ This implies that if } |t - t'| < \delta, |f(t) - f(t')| = |\lim_{\epsilon \to \epsilon_0} (g(\epsilon, t) - g(\epsilon, t'))| \le \delta$$

 $\Delta$ . It also implies that if  $|\epsilon - \epsilon'| < \delta$ ,  $|h(\epsilon) - h(\epsilon')| \le \max_{t \in T} |g(\epsilon, t) - g(\epsilon', t)| < \Delta$ . Since f is continuous and h is uniformly continuous, both sides in Eq. (S75) are well-defined.

Since  $(L.H.S.) \ge (R.H.S.)$  is trivial, we show the converse. For any  $\Delta > 0$ , there exists  $\delta > 0$  such that  $|f(t) - g(\epsilon, t)| < \Delta$  if  $|\epsilon - \epsilon_0| \le \delta$  for any  $t \in T$  and  $\epsilon$ . Thus, we obtain

$$\lim_{\epsilon \to \epsilon_0} \max_{t \in T} g(\epsilon, t) \le \lim_{\epsilon \to \epsilon_0} \max_{t \in T} (f(t) + \Delta) = \max_{t \in T} \lim_{\epsilon \to \epsilon_0} g(\epsilon, t) + \Delta. \tag{S76}$$

Since this holds for any  $\Delta > 0$ , this completes the proof.